CRUISE-DASH OPTIMIZATION APPLIED TO AN AIR-BREATHING MISSILE

by

David F. Chichka

Thesis submitted to the Faculty of the

Virginia Polytechnic Institute and State University

in partial fulfillment of the requirements for the degree of

Master of Science

in

Aerospace and Ocean Engineering

APPROVED:

E. M. Cliff, Chairman

H. J. Kelley

F. H. Lutze

December, 1985

Blacksburg, Virginia

CRUISE-DASH OPTIMIZATION APPLIED TO AN AIR-BREATHING MISSILE

by

David F. Chichka

E. M. Cliff, Chairman

Aerospace and Ocean Engineering

(ABSTRACT)

The method of singular perturbations is applied to the determination of the optimal range-fuel-time trajectory for an air-breathing missile. This method is shown to lead to the reduced-order "cruise-dash" model, and this model is used in the optimization study. Earlier work in this area is extended by the inclusion of two not heretofore considered limits on the dynamical system.

The results of the earlier work are shown to hold throughout much of the velocity regime in which the missile operates, but operation in the very high and very low velocity ranges is shown to be sharply curtailed, with the optimal operating points being changed drastically in some cases. Also, the effect of the non-zero minimum admissible throttle setting and the resultant throttle-chattering on the solution of the control problem is examined in some detail.

ACKNOWLEDGMENTS

I am indebted to Dr. E. M. Cliff for his constant interest, his guidance, and his invaluable suggestions in furthering this work. I am equally indebted to Uday Shankar, who interpreted these suggestions for me. I also wish to thank Drs. H. J. Kelley and F. H. Lutze, who served on my committee.

I wish to take this opportunity to thank all my friends for their support, moral and otherwise. In particular, I wish to thank Karl Bilimoria for his help, Dean Sparks for the reams upon reams of notes from class after class that he allowed me to copy after I had slept soundly and securely as he toiled away, and Greg Strauch because his perspective on all this kept mine from becoming absolutely Dantean.

And, of course, there aren't enough thanks in all the world for Anita.

NOMENCLATURE

ENGLISH SYMBOLS

C_N ..... Normal force coefficient

C_X ..... Axial force coefficient

D ..... Drag

E ..... Energy-height

g ..... Acceleration due to gravity

H ..... Hamiltonian

h ..... Altitude

J ..... Performance index

L ..... Lift

M ..... Mach number

Q ..... Fuel-flow rate

R ..... Range

T ..... Thrust

t ..... Time

V ..... Velocity

W ..... Weight

GREEK SYMBOLS

α ..... Angle-of-attack

β ..... Inequality constraint

γ ..... Flight-path angle

$\varepsilon, \varepsilon^1, \varepsilon^2$ ..... Interpolation parameters

η ..... Throttle-setting

$\lambda_{()}$ ..... Costate variable

$\mu_{()}$ ..... Weight in performance index

ψ ..... End condition

SUPERSCRIPTS

$\dot{}$ ..... Time derivative

* ..... Optimal

— ..... Specified

SUBSCRIPTS

c ..... Chattering, circular orbit

e ..... Equilibrium

eo ..... Engine-out

F ..... Fuel

f ..... Final

T ..... Time, terrain

TABLE OF CONTENTS

CHAPTER 1: INTRODUCTION 1

CHAPTER 2: PROBLEM FORMULATION AND ORDER REDUCTION . . 3

Performance Index 3

System Dynamics 5

Order Reduction 8

CHAPTER 3: SOLUTION PROCEDURE 13

Necessary Conditions 13

Computational Procedure 14

Numerical Evaluation of $Q^*(V)$ 16

CHAPTER 4: RESULTS OF NUMERICAL ANALYSIS 23

Comparison of Results for Constrained and Unconstrained Case 23

General Results 26

Chattering Throttle 31

CONCLUSION 36

Discussion of Results 36

Suggestions for Further Work 37

REFERENCES 39

APPENDIX A. AERODYNAMIC/PROPULSIVE MODELING 41

Atmosphere 41

Aerodynamics 41

Propulsion 42

VITA 71

LIST OF ILLUSTRATIONS

Figure 1. Calculation of chattering throttle-setting. 45

Figure 2. Flight Envelope. 46

Figure 3. $Q^*(V)$ for typical cases. 47

Figure 4. Throttle-Setting for $Q^*(V)$ for typical cases. 48

Figure 5. Fuel economy for $Q^*(V)$ for typical cases. . 49

Figure 6. Altitude for $Q^*(V)$ for typical cases. . . . 50

Figure 7. Characterization of results. 51

Figure 8. $Q^*(V)$ vs. V with lines of constant H (λ_F large). 52

Figure 9. $Q^*(V)$ vs. V with lines of constant H (λ_R large). 53

Figure 10. $Q^*(V)$ vs. V with supporting hyperplane. . . 54

Figure 11. $Q_s(h)$ for fixed V. 55

Figure 12. Variation of T-D and η^* with altitude (fixed V). 56

Figure 13. Partial derivative of Q w.r.t. h vs. h (fixed V). 57

Figure 14. η^* vs. h (fixed V). 58

Figure 15. Fuel-flow rate vs. altitude (fixed V). . . 59

Figure 16. Air density vs. altitude. 60

Figure 17. Sonic velocity vs. altitude. 61

Figure 18. Normal Force Coefficient vs. Alpha (low M). 62

Figure 19. Normal Force Coefficient vs. Alpha (high M). 63

Figure 20. Normal Force Coefficient vs. M (alpha fixed). 64

Figure 21. Axial Force Coefficient vs. Alpha (M fixed). 65

Figure 22. Axial Force Coefficient vs. M (alpha fixed). 66

Figure 23. Capture Ratio vs. Mach number. 67

Figure 24. Thermal Choke Limits on Throttle-Setting. . 68

Figure 25. Thrust Specific Impulse (fixed M, h) . . . 69

Figure 26. Inlet Drag Increment vs. M. 70

CHAPTER 1: INTRODUCTION

Advanced missile technology, featuring throttleable air-breathing engines, offers the possibility of long-range intercept of incoming threats. The task of making efficient use of the throttle capability presents a challenging problem to both the flight control designer and the combat-systems analyst. The additional flexibility provided by the throttle allows for a trade-off of range against velocity. In general, one expects that reducing the velocity will result in an increase in the achievable range.

This flexibility naturally leads to the idea of tailoring the flight speed to the actual situation in the combat scene. The fire-control logic should take into account the missile's range/velocity capability and balance it against the current target information in selecting the appropriate average speed for the mission. The selection would then be supplied to the missile, perhaps as part of the pre-launch initialization.

In principle, of course, the information could be transmitted to the missile in flight. Indeed, the fire-control system may wish to update the choice of velocity as further target information becomes available. Whatever the details of the fire-control procedure, it is clear that a basic requirement is a good estimate of the range/speed capability

of the missile, along with a missile controller capable of implementing any of the range/speed combinations selected.

Given these requirements it seems natural to seek the maximum range for a given average speed. If this can be determined, and the the flight-control to achieve it characterized, the missile can be employed in an optimal fashion. A system with these capabilities would be able to achieve intercepts beyond the abilities of other systems.

This thesis summarizes the results of a preliminary study of optimal time-fuel-range flight for an airbreathing missile. The next chapter presents the problem formulation. The dynamical model is presented, as are the constraints upon the system. The concept of reduced-order modeling is introduced and applied to the problem at hand.

Chapter Three presents the solution procedure and describes the construction of the numerical procedure used in the study. Results are discussed qualitatively in Chapter Four. In particular, the effects of limits on the throttle-setting and on the flight envelope are treated. Also discussed are the results of the non-zero minimum throttle-setting, which leads to the phenomenon of "chattering" to achieve effective settings below this minimum. Finally, the conclusions of the study are presented in Chapter Five, along with some recommendations for further work.

CHAPTER 2: PROBLEM FORMULATION AND ORDER REDUCTION

In this chapter the cruise-dash problem is defined in the form of standard optimization practice [1, 2]. First a performance index is chosen. The dynamical system is then described, along with the constraints on it. Finally, the order-reduction technique is introduced and applied.

PERFORMANCE INDEX

As mentioned in the preceding chapter, the purpose of this study is to characterize the trade-off of velocity and range that is possible with a variable throttle. This in itself does not well define the performance index to be considered. There are in general several ways in which the cost function might be specified [3].

One approach might be to attempt the minimization of a weighted sum of time and fuel required to achieve a specified range. In this case the cost function would be written

$$J = \mu_T t_f + \mu_F W_F(t_f)$$

where μ_T and μ_F are specified (positive) weights, t_f is the final time, and W_F is fuel consumed. The end conditions would include

$$\psi = R(t_f) - \bar{R}_f = 0$$

where $\bar{R}_f$ is the desired range at t_f. By varying the values of μ_T and μ_F one could alter the relative importance of time and fuel economy. With μ_T/μ_F large, the final time is the dominant factor and the average speed will (presumably) be large. With μ_T/μ_F small, the fuel economy will be stressed and the velocity would be expected to be somewhat lower.

Alternatively, one could define a cost function

$$J = \mu_T t_f - \mu_R R(t_f)$$

with one of the end conditions being

$$\psi = W_F(t_f) - \bar{W}_{Ff} = 0$$

Here, the weights μ_T and μ_R define a trade-off between time and range for a specified amount of fuel used.

Finally, the cost function could be defined

$$J = -R(t_f)$$

with end-conditions including

$$\psi_1 = W_F(t_f) - \bar{W}_{Ff} = 0$$

$$\psi_2 = R(t_f) - (\bar{V} \times t_f) = 0$$

Using this formulation the objective is to maximize range while using a specified amount of fuel ($\bar{W}_{Ff}$) and attaining a specified average speed ($\bar{V}$).

Intuitively, it would be expected that these formulations are identical. That is to say, that combinations of weights could be found in each case that would duplicate the results found by using each of the other cost functions. This is in fact not the case. It is shown in Ref. 3 that the problems

are similar but not identical. For a more complete discussion, the reader is referred to [3].

For this study, the cost function chosen is of the second type. Thus, the problem is to minimize the quantity

$$J = \mu_T t_f - \mu_R R(t_f)$$

while using a specified amount of fuel.

SYSTEM DYNAMICS

To study the best-range problem one needs a dynamical model of the missile. For the purposes of trajectory optimization, a point-mass model is sufficient [4]. The full-order model (prior to the order-reduction discussed below) used in this study is such a model, based on Newtonian mechanics. Rigid-body motions are ignored, as are any structural vibrations.

The model used allows only for planar flight, without crossrange components of velocity or acceleration. The three-dimensional model results in a more complex problem, and has not been considered here. The basic equations of the model used are

$$\begin{aligned}
\dot{h} &= V\sin\gamma \\
\dot{\gamma} &= \frac{g}{V}\left\{\frac{L}{W} - \left[1 - \left(\frac{V}{V_c}\right)^2\right]\cos\gamma\right\} \\
\dot{E} &= (T - D)V/W \\
\dot{R} &= V\cos\gamma \\
\dot{W}_F &= Q
\end{aligned} \tag{1}$$

where the state variables are the altitude h, the flight-path angle γ, the specific energy E (discussed in the Order Reduction section below), the distance covered R, and the weight of fuel consumed W_F. Here V is the vehicle velocity, L and D are the standard aerodynamic forces lift and drag, respectively, T is thrust, and Q denotes fuel-flow rate. Also included is the centrifugal-relief term (V/V_c), where V_c is the (constant) circular orbit speed at one Earth radius. The constant g is the acceleration due to gravity.

To complete the description it is necessary to specify the functional dependence of the aerodynamic forces L and D and the propulsive characteristics T and Q. While full details are left to Appendix A, it is noted that the model assumes that L and D are functions of V, h, and the vehicle angle-of-attack α, while T and Q are functions of V, h, and the throttle-setting η.

In addition to the missile dynamical equations, the system is subject to a set of inequality constraints. These might typically include limits due to terrain, dynamic pressure, propulsive limits, structural load limitations, and/or aerodynamic limitations. For this problem, there were four such limits considered:

$$\beta_1 = (h - h_T) \geq 0 \qquad \text{(terrain limit)}$$

$$\beta_2 = (\alpha_{max} - \alpha) \geq 0 \qquad \text{(aerodynamic limit)} \qquad (2)$$

$$\beta_3 = (h - \bar{h}(M)) \geq 0 \qquad \text{(Mach-altitude limit)}$$

$$\beta_4 = (\eta_{max}(h,M) - \eta) \geq 0 \qquad \text{(propulsive limit)}$$

The aerodynamic limit in this problem is expressed as a maximum allowable angle-of-attack, constant over Mach number and altitude. This limit prevents choosing an optimal trajectory that is beyond the capabilities of the vehicle. In numerical simulation, it has the added virtue of preventing the data tables based upon angle-of-attack from being exceeded. In many cases, the aerodynamic limit is expressed as an upper limit on the value of lift coefficient [5]. This has the same result.

The Mach-altitude limit may reflect any or all of the several considerations which can be expressed as a function of h and M. For example, a limit on the maximum allowable dynamic pressure can be written in this way. Also, limits on the maximum stagnation pressure and stagnation temperature may be expressed by such a function. In this problem, the Mach-altitude limit is expressed as a specified tabular function, which may include any number of these.

The last constraint is due to the limit on heat addition to an airstream. As heat is added to a supersonic flow, such as in the combustion chamber of the engine, the Mach number goes down. After a certain amount of heat has been added, the flow has reached a Mach number of one, and further heat

addition will result in unsteady flow, with internal shocks generated [12]. Such a flow is referred to as choked, and for this reason β_4 is referred to as a thermal-choke limit.

In this case, the airflow involved is the flow in the engine combustion chamber, and the heat is added through the burning of fuel. The prediction of the amount of fuel that could be added before choking the flow would involve the engine geometry, the external conditions (Mach number, temperature, etc.), the combustion efficiency, and several other factors. This was not done in the present study; rather, a table of maximum throttle-setting (η_{max}) values as a function of h and M was used. This table was interpolated using a cubic spline-lattice approximation.

In this study, two cases were considered. In the first, referred to as the unconstrained case, the Mach-altitude and thermal-choke limits were not taken into account. These limits were considered in the constrained case. The terrain limit and the maximum angle-of-attack limit were always considered. The methods used to calculate these four limits are described in Appendix A.

ORDER REDUCTION

The classical approach at this point in the solution process would be to construct the pseudo-Hamiltonian, with its Lagrange multipliers [1]. From this the Euler equations

would be derived, and the resulting tenth-order system solved as a two-point boundary-value problem. This approach is conceptually straight-forward, but in the application encounters certain difficulties. Foremost among these is the computational instability of the system [4, 5].

To overcome this difficulty, the concept of reduced-order modeling is often introduced. In this approach the original problem is broken down into two or more lower-order problems on different time-scales. This is based on the observation [6] that certain variables in the equations of motion change much faster than others.

Reduced-order models ignore the dynamics of the changes of these "fast" variables, making them much simpler and computationally much more tractable. The results obtained by such a model are, of course, approximate, and are called reduced-order solutions. If the fast dynamics of the system have only a minor effect on the behavior, the reduced-order solution will closely follow the exact solution, except in the neighborhood of the end-points [5, 8, 9], or at "turning points" in the trajectory [11].

It is for this reason that the energy-height E is used as a state variable rather than the more familiar velocity V. This method of modeling the system in trajectory analysis has been in use for some time [3 - 9]. The major reason for using E in these applications is the time scale in which it moves. One may think of it as an "intermediate" variable, while h

and γ are "fast" and R and W_F are "slow". That is to say that h and γ change much faster than E, while R and W_F change much more slowly.

This observation leads to the use of singular-perturbation theory in trajectory analysis [3, 5, 8, 9]. This approach was first used by Kelley [8], and this analysis will closely follow his methodology.

The first step in the reduction method is the recasting of the dynamical system, adding interpolation parameters. The system (1) so recast is

$$\begin{aligned}
\varepsilon^2 \dot{h} &= V\sin\gamma \\
\varepsilon^2 \dot{\gamma} &= \frac{g}{V}\left\{\frac{L}{(W_0 - \varepsilon W_F)} - \left[1 - \left(\frac{V}{V_c}\right)^2\right]\cos\gamma\right\} \\
\varepsilon^1 \dot{E} &= \frac{(T - D)V}{(W_0 - \varepsilon W_F)} \qquad (3) \\
\dot{R} &= V\cos\gamma \\
\dot{W}_F &= Q
\end{aligned}$$

Note that weight has been defined by $W = W_0 - \varepsilon W_F$, where W_0 is the initial weight of the missile. Here ε is an interpolation parameter as mentioned above. When $\varepsilon = 1$, the equation becomes the standard $W = W_0 - W_F$. However, as $\varepsilon \to 0$, the influence of W_F decreases, and in the limit the weight becomes constant.

This is precisely the manner in which ε^1 and ε^2 are used. These are interpolation parameters, with the defined property that ε^2 approaches zero much faster than does ε^1. This reflects the time-scale classification of the state variables.

The altitude h and flight-path angle γ occupy the fastest scale, the specific energy the next-fastest, and range and W_F the slowest.

In the application of the singular perturbation technique, these interpolation parameters are allowed to approach zero. As ε^2 approaches zero the first two equations in (3) become equality constraints, requiring that γ equal zero and lift equal weight. This is known as the energy-state approximation [5]. As ε^1 also becomes zero, the third equation also forms an equality constraint, requiring that thrust equal drag in level flight. This form of the model is known as the cruise-dash approximation, and this is the formulation used in this study. [Note: The statement that lift equal weight is not completely accurate. The constraint is actually that lift equal the weight as modified by the centrifugal-relief term. This modification is very small, and may generally be ignored. For the remainder of this discussion, it will be understood that the vehicle weight includes this small term.]

Note that in this formulation, the velocity V is thought of as a quantity defined in terms of the altitude and energy-height as

$$V = [2g(E - h)]^{1/2}.$$

This establishes h, E, and V as a trio of interdependent variables, with the third defined by the other two.

Though the order-reduction technique takes the derivatives of the altitude and specific energy as negligible, this is

not to imply that they are constants. Rather, they are considered as "control-like", which is to say that they are chosen by the analyst and can change instantaneously in the reduced-order model. (Note that while γ is in the "fast" time-scale, it is zero in the reduced-order model.)

To summarize, the problem being attacked, after order-reduction to the cruise-dash model, has taken the form:

Minimize the weighted sum of time-of-flight minus distance covered

$$J = \mu_T t_f - \mu_R R(t_f) \tag{4}$$

while using a specified amount of fuel $\bar{W}_{Ff}$, for the system

$$\begin{aligned} \dot{R} &= V \\ \dot{W}_F &= Q \end{aligned} \tag{5}$$

subject to the constraints

$$\begin{aligned} L &= W \\ T &= D \end{aligned} \tag{6}$$

while remaining within the boundaries defined by the inequality constraints (2).

CHAPTER 3: SOLUTION PROCEDURE

In this chapter the problem as formulated in Chapter 2 is approached from a variational standpoint. The necessary conditions for an optimal solution are considered, and the computational approach is discussed.

NECESSARY CONDITIONS

In the cruise-dash formulation, the problem is to find the controls to take the system from an initial point to an unspecified final point at an unspecified final time in such a mannner as to minimize the performance index (4). Recall that of the trio of variables h, E, and V, any two can be thought of as the control variables, with the third specified by the values of those two. In this discussion, the variables h and V will be used.

To solve the problem as stated, one first forms the variational Hamiltonian:

$$H = \lambda_R V + \lambda_F Q$$

Since the state variables R and W_F do not appear in the Hamiltonian, the Euler-Lagrange equations imply that λ_R and λ_F are constant in time. Also, as time does not appear explicitly in the Hamiltonian, it is constant in time [1].

The terminal transversality condition [1] requires that

$$\lambda_{x_j}(t_f) = \left.\frac{\partial J}{\partial x_j}\right|_{t_f}$$

for all x_j unspecified at t_f, and that

$$\left(\frac{\partial J}{\partial t} + H\right)_{t=t_f} = 0.$$

In this problem, the range R is unspecified at t_f, while the final weight of fuel consumed is specified. Therefore the transversality condition becomes

$$\lambda_R = -\mu_R$$

and

$$H = -\mu_T$$

From these conditions, a bit of algebra shows that the (constant) multiplier λ_F can be solved for:

$$\lambda_F = [\mu_R V(t_f) - \mu_T]/Q(t_f).$$

The Minimum Principle [1] requires that the optimal solution minimize the Hamiltonian. Thus the control problem can be thought of as seeking the point on the h, V plane which minimizes H.

It should be noted that a mathematically rigorous derivation of these conditions would involve the Hamiltonian of the original system with interpolation parameters. That the approach used here is equivalent is shown in Kelley [8].

COMPUTATIONAL PROCEDURE

Inserting the functional dependence of Q into the results of the preceding section, one can define the quantity

$$H = \lambda_F Q(\eta,h,V) + \lambda_R V.$$

The objective now becomes to find a point within the flight envelope as defined by the constraints (2) which minimizes this quantity, subject to the constraints of steady, level flight (6).

As stated, this is apparently not a particularly straight-forward problem. However, recalling the functional dependencies of the various aerodynamic and propulsive quantities as stated in Chapter 2 and utilizing the restrictions (6), a more workable problem can be constructed.

For a given h,V pair, the angle-of-attack is found for which $L(h,V,\alpha) = W$, in keeping with the lift-equal-weight constraint. This then defines the drag $D(h,V,\alpha)$. From this information, one proceeds to solve $T(h,V,\eta) = D$ for the throttle-setting η. This is all the information needed to define $Q(\eta,h,V)$. In this way, the fuel flow Q may be thought of as a function of h and V, and so in turn may H.

To continue with the analysis, note that the second term in H depends only upon V. Since

$$\min_{h,V} H(h,V) = \min_{V}\left[\min_{h} H(V,h)\right]$$

this leads to the idea of minimizing the fuel-flow over admissible altitudes for fixed V. Thus, define

$$Q^*(V) = \min_{h} [Q(\eta,h,V)]$$

and

$$H^*(V) = \lambda_F Q^*(V) + \lambda_R V.$$

Now, the problem can be restated as seeking the velocity V that minimizes H^*.

NUMERICAL EVALUATION OF $Q^*(V)$

The function $Q^*(V)$ is evaluated by performing a one-dimensional minimization over altitude for given velocity. The velocity is held fixed for each individual minimization. The computation of Q^* for the particular velocity is a conceptually straight-forward procedure, although the actual process is somewhat intricate.

The procedure used assumes that there is a single interval of altitudes to be examined in the minimization for each fixed velocity. To ensure this, it is necessary to show that the inequality constraints (2) define such an interval for each velocity in the range of interest. One way to do this is to show that each constraint results in a single semi-infinite interval, bounded either above or below but not both.

In the case of β_1, the terrain limit, this property is obvious, as h_T is constant for all V. In the case of the maximum angle-of-attack limit (β_2), it is assumed that the angle-of-attack required to maintain straight and level flight at a fixed velocity increases with altitude. Under this assumption, β_2 also has the requisite property. These two limits give the lower and upper bounds on the interval to be examined when the Mach-altitude limit (β_3) and the thermal-choke limit (β_4) are not considered.

When these two further limits are considered, the first two are still taken into account. However, the interval they define may be further reduced by β_3 and β_4.

The Mach-altitude limit provides some difficulty because it is expressed as minimum altitude with Mach number as the independent variable. M is not one of the state variables, and is dependent upon altitude. Thus there is no certainty that the limit is indeed a well-defined function in terms of velocity.

Since M is a function only of h and V, any point (h,M) satisfying $h = \bar{h}(M)$ can be expressed as a point (h,V). However, due to the variation of speed of sound over altitude, a function $\bar{h}(M)$ may in fact not define an "equivalent" function $\tilde{h}(V)$. For some values of V, there may be multiple values of h for which the (h,V) point corresponds to an (h,M) point satisfying $h = \bar{h}(M)$. This possibility must be taken into account in the computational procedure, either by showing that there is a unique solution (h,V) for all V in the range of interest, or by checking for multiple solutions during the computations.

As mentioned above, the Mach-altitude limit in this problem is expressed as a tabular function. The function was fit by a cubic spline, and a continuous representation achieved. This representation was then mapped into the h,V plane and shown to be a well-defined function. Thus it was possible to express the limit as a simple function of airspeed. Had

this not been the case, it would have been necessary to allow for multiple subintervals within the interval defined by β_1 and β_2.

As with the Mach-altitude limit, the thermal-choke limit is supplied as a function of altitude and Mach number. In this case, both of these are independent variables, however, and as every point (h,M) has a unique representation in the h,V plane, the function $\eta_{max}(h,M)$ is also a well-defined function in h and V, and can be used in this formulation without trouble.

The range of altitudes to be examined having been determined, the procedure performs the minimization using a grid-search algorithm. The altitude range is scanned using a specified step size and the value of Q at each point calculated. The region surrounding the point producing the lowest such value found is then examined, using a reduced step size. When the interval containing the minimum has been so reduced a specified number of times, an IMSL routine [13] is used to find the precise minimum within that interval.

As mentioned in the preceding section, for a fixed V, specifying h is enough to define the angle-of-attack, utilizing the requirement that lift equals (the known) weight. The upper limit on altitude guarantees that such an angle-of-attack can be found that satisfies the aerodynamic limit. From this angle-of-attack and the values of h and V the drag is calculated as described in Appendix A.

The knowledge of the drag value, coupled with the knowledge of h and V, is sufficient to allow "solving" for the fuel-flow rate at that h,V point. For brevity, the actual equations are left to Appendix A. Only the method will be described here.

The stoichiometric fuel-flow rate Q_s is defined fully by the values of h and V, and the actual fuel-flow rate Q(h,V) is the product of this value and the throttle-setting η. The value of η is then either an equilibrium setting (denoted η_e), at which $T(h,V,\eta) = D$, or it is a chattering setting (denoted η_c), which will be discussed below. As Q_s is fixed by the h,V point, and the objective is to minimize Q, the lowest possible value of η is desired.

At a specified h,V point, the thrust is modeled as a cubic function of η. As the drag has no dependence on η, this allows the the equilibrium throttle-setting to be solved for by solving the "T - D cubic," the equation $T(\eta) - D = 0$. If a setting can be found to satisfy this equation, this value is assigned to η_e. Because the thrust is modeled as a cubic, it is theoretically possible that as many as three values may be found to satisfy the equation. In such a case, the lowest value would be used as η_e.

The candidate values for η_e must lie within the admissible range, which is constrained on both the lower and upper ends. The upper limit is the lowest of the nominal limit unity, the limit due to the maximum fuel-flow rate (described in Appen-

dix A), and the thermal-choke limit in the constrained case. The lower limit is a non-zero minimum value η^0, below which the engine will not function. This value is constant for all h and V. This does not enter into the system of inequality constraints (2) because the calculated throttle-setting may be a chattering setting below this value.

"Chattering" comes from the idea of time-sharing between two settings to achieve an average performance between the two [10]. In the case of throttle-setting, this refers to flying for some time at a setting for which thrust exceeds drag, and for some time at a lower value. There is nothing in the model to prevent the shifting between the two settings from being instantaneous, and therefore it is mathematically possible to achieve a constant average setting between the two points by "chattering;" i.e., switching at infinite rate between them. It is this constant average setting which is referred to as the chattering setting.

Consider the situation as shown in Figure 1. The figure shows the T - D curve plotted against η. The curve is entirely above the η axis, meaning that there is no equilibrium throttle-setting. However, it is possible to calculate a chattering setting η_c that will have the effect of an equilibrium setting.

As the entirety of the T - D curve is above the η axis, any point on the curve could be used as the upper chatter point. The average setting is found simply by drawing the

line from the upper point to the point (0, $-D_{eo}$), where D_{eo} is the engine-out drag. Where this line crosses the η axis is the η_c.

As the desire is to find the minimum fuel-flow, it is necessary to find the minimum η_c. It is clear from the figure that the point of intersection of the line and the η axis will move to the left as the angle θ on the figure increases. As θ is always less than 90 degrees, its tangent increases as it does. Thus the mathematical approach to minimizing η_c is identical to maximizing $\tan\theta$ over admissible values of η.

Since the upper end of the chatter line must be on the T - D curve, and the T - D curve is described by a cubic in η, the tangent of θ can be expressed as a quartic in η. The derivative of this is then a cubic, which is solved for possible maxima. These maxima are candidate values of η at the upper chatter point. To these possibilities is added the value η^0, should $T(\eta^0)$ be greater than drag. All of the possibilities that lie within the admissible region are examined for the values of the η_c they generate, and the lowest of these is used as η_c in the minimization procedure.

Once the candidates η_e and η_c are calculated (if they exist), the lowest of them is taken to be the throttle-setting for the h,V point under consideration. This value is then multiplied by Q_s, and the product is the value Q(h,V) for that point. Should no admissible value of η be found, Q is set to a very large number. The grid-search routine then

goes on to the next h for the fixed V under consideration, and the process is repeated until the minimum value of Q(h,V) is found. This minimum value is Q^* at that V.

CHAPTER 4: RESULTS OF NUMERICAL ANALYSIS

This chapter presents the results of the numerical study. In the first section, the results for the constrained and unconstrained cases are compared, and the effects of the Mach-altitude and thermal-choke limits are discussed. The second section presents a method of characterizing the results in terms of the multipliers in the Hamiltonian, and demonstrates that for certain values of these multipliers the solution to the optimization problem is not unique. The third section then discusses the effect of the non-zero minumum admissible throttle-setting on the solution, and the attendant throttle-chattering.

COMPARISON OF RESULTS FOR CONSTRAINED AND UNCONSTRAINED CASE

The most obvious effect of the additional limits considered in the constrained case is the reduction in the flight envelope. This is shown in Figure 2, in which the lightly shaded region represents the constrained flight envelope. The dashed curves represent the limits due to propulsive considerations, and the solid curves show the limits due to the Mach-altitude limit and the aerodynamic limitations. The cross-hatched area is the chattering region, in which the imposition of the thrust-equal-drag constraint requires a

chattering throttle-setting, as discussed in the preceding chapter.

The unconstrained flight envelope effectively has no right-hand limitation, as the propulsive data tables are exceeded long before the two dashed lines near each other. It is worthy of mention that, in this region, the thermal-choke limit has no effect; it is felt only at low Mach numbers.

The constrained flight envelope not only has a sharply limited right-hand boundary, but the low-velocity region to the left is also reduced, although not as drastically. The dashed curves in Figure 2 are the limiting altitudes for flight with the thermal-choke limit in effect. The finely-shaded region represents the additional h,V area attainable if the thermal-choke limit could be ignored. This region extends only the low-velocity boundaries of the envelope since, as mentioned above, the thermal-choke limit has no effect at higher velocities.

With the flight envelope in mind, consider Figures 3 - 6. These show $Q^*(V)$, the corresponding optimal throttle-setting, the fuel economy (in distance covered per unit mass of fuel consumed), and the altitude for optimal flight, respectively, for both the constrained and unconstrained cases. In each case, the constrained curve (represented by the solid line) follows the unconstrained through most of the velocity range, with variations in the low-velocity and high-velocity regions.

The variations at the high-velocity portion of the curve are easily understood in terms of the reduced flight envelope. In Figure 6, note that the constrained curve takes a sharp upturn in altitude away from the unconstrained curve, but almost immediately ends. This corner is the result of the curve encountering the Mach-altitude limit as velocity is increased. The point of intersection is very near the right-most limit of the flight envelope, and the altitude soon reaches the absolute limit. The unconstrained curve simply runs on until the highest velocity desired has been examined.

At the low velocity end of the curve, the result of the thermal-choke limit is most easily seen in Figure 4. In this case, the unconstrained function runs in a smooth curve from a high value at the lowest velocity to a local minimum, and then runs with a general upward trend throughout the rest of the velocity range. The constrained curve, on the other hand, runs along the upper boundary of the chattering region for a short distance, then jumps to another function, defined by the thermal-choke limit, and follows that until the unconstrained curve is joined.

The portion of the curve defined by the thermal-choke limit is against the upper edge of the constrained flight envelope. This is a result of the thermal-choke limit decreasing with altitude for fixed V, while the throttle-setting required for steady flight increases with altitude.

The effect of the throttle constraint on the other parameters is easily seen from the other figures. From Figure 3 it is seen that the result is a large increase in fuel-flow, and the other figures show that it also means flight at a much lower altitude (Figure 6) and with much less fuel economy (Figure 5).

Among the most interesting points to consider from these graphs is that in no circumstance was a chattering throttle-setting found to be the optimal, despite the minimum setting being followed at the lowest velocities. The reasons for this are examined in detail below. First, however, the generic nature of the optimal solutions is discussed.

GENERAL RESULTS

Recall that the objective of the procedure is to find the value of velocity for which

$$H^* = \lambda_F Q^*(V) - \lambda_R V$$

is minimized. Recall also that $Q^*(V)$ is the <u>minimum</u> value of Q for that V. Flight can also be maintained at values of Q greater than Q^*, for some range of Q limited by the system equations. Flight can not be maintained, however, at values of Q below $Q^*(V)$.

Figure 7 shows the $Q^*(V)$ curve for the constrained case from Figure 3. Also shown in the figure are lines of constant H^*, for constant λ_F and λ_R. The slope of these lines is

λ_R/λ_F. The value of H^* decreases with increasing velocity (recall that λ_R is non-positive), and with decreasing Q. Were the values of the multipliers changed to reflect greater emphasis on minimizing Q than on maintaining a high average speed (λ_R/λ_F approaching zero), the lines of constant H^* would be more nearly horizontal (Figure 8). Were they changed to place more weight on high speed, the lines would rotate toward the vertical (Figure 9). Note that with the lines horizontal the optimal point is at the global minimum, and as λ_R/λ_F increases, it moves to the right. As the slope cannot be negative, the optimal operating point will never be to the left of the global minimum.

For any admissible combination of λ_F and λ_R, such a family of lines of constant H^* will exist. In general, flight at any particular value of H^* for that combination will be possible at the point or points on the Q, V plane at which the line corresponding to that value of H^* intersects the $Q^*(V)$ curve, and at points along at least some segments of the line above the curve, should portions of the line be above the curve.

As it is desired to minimize H^*, the actual range of achievable fuel-flow rate above Q^* is not of interest, since H^* decreases as Q decreases. Therefore, the optimal operating point for any specified pair λ_F and λ_R will be on the $Q^*(V)$ curve.

As H^* decreases as Q decreases, there will be no points on the $Q^*(V)$ curve below the line of minimum attainable H^* Thus the line of constant H^* with this value will separate the portion of the plane with achievable operating points from the portion which contains no such points. Such a surface is referred to as a "supporting hyperplane" in optimization theory [3].

If the supporting hyperplane has only one point of contact with the $Q^*(V)$ curve, this point is the unique solution to the control problem. This is the case in Figures 7-9. However, should the supporting hyperplane have multiple points of contact, there is an equally optimal solution at each of these points. This is the case in Figure 10, in which the supporting hyperplane has two points of contact, each of them equally optimal. (Note that this is true also for the unconstrained solution, as the interesting portion of the curve falls in the range in which the solutions are identical.)

To further demonstrate the implications of the nonconvexity of the $Q^*(V)$ curve, consider the case in which λ_R is increased in relation to λ_F. This causes the lines of constant H^* to rotate in a counter-clockwise direction on the $Q^*(V)$ - V plane. (This might correspond to the case of a rapidly approaching target, in which as the firing of the missile is delayed the speed of the missile becomes much more desireable than its range, as the distance it must cover decreases.)

If the slope begins at a low enough value, the optimal operating point is on the low-velocity portion of the curve (Figure 8). As the value of λ_R/λ_F passes that at which there are two points of contact, the optimal point jumps to the high-velocity portion of the curve (Figure 9). The optimal point never occupies the central portion of the curve.

A related consequence of this non-convexity is illustrated when the problem of minimum-fuel operation at a specified average velocity is considered (recall that this was one possible formulation of the performance index for this problem). The obvious solution approach would be to simply calculate the altitude for which fuel-flow is a minimum at that velocity. Note that this is precisely $Q^*(V)$.

Referring to Figure 10, it is seen that quite a large range of velocities is included in the area of non-convexity. Should the desired average speed fall in this range, it is obvious that the "optimal" solution given by the classical approach would give poorer performance than the point on the hyperplane at that velocity.

The velocity V_1 on Figure 10 corresponds to the lower point of tangency; V_2 the higher. Note that the value of $Q^*(V)$ at the specified velocity (called V_0 henceforth) can be achieved by flying for some time at V_1 and some time at V_2, with the time apportioned so as to average V_0. This simple time-sharing operation will give an average velocity of V_0 for the overall trajectory. Since V in the cruise-dash

model can change instantaneously, it is mathematically possible to achieve constant average speed V_0 by "chattering" between V_1 and V_2.

Referring back to Figure 3, one can see that the results of the control problem will be identical for both the constrained and unconstrained cases when the value λ_R/λ_F is low, and the optimal solution is on the low-velocity portion of the curve. This is because the absolute minimum of $Q^*(V)$ is on the section of the curve that is the same for the two cases. The thermal-choke limit is not active at these Q^* - V points.

The case is quite different at the high-velocity end of the curve. As has been noted, as λ_R/λ_F increases, the optimal operating point moves to the right along the curve. Once this point reaches the maximum velocity, however, it can no longer move, and the solution remains constant as the slope of the lines of constant H^* increase.

It is to be expected that this would also occur at some limiting velocity for the unconstrained case. Numerically, however, there is no such limiting velocity, and the data tables in the model may be extrapolated almost without end (results were found at velocities as much as 1.5 times the limiting velocity in the constrained case). These extrapolated results must be considered physically meaningless, of course, yet there is nothing in the model to prevent points in these ranges from being chosen by the procedure.

CHATTERING THROTTLE

The concept of chattering throttle has particular significance in this problem due to the non-zero minimum throttle setting for sustained engine operation (η^0). As described in Chapter Three, a setting lower than this value may be achieved through throttle-chattering.

Referring back to Figure 4, the optimal throttle setting for the constrained case is equal to η^0 between the points marked A and B on the curve. This form of the curve was found to be the result for all constrained cases run, with the only difference being that the velocity at B (V_b) is dependent upon the vehicle weight. For velocities less that V_b, the minimization of Q over h for fixed V (as described in Chapter Three) always finds the minimum at η^0.

The explanation for this avoidance of the chattering throttle settings is based upon the standard mathematical requirements for the minimum of a continuous function. That is to say, the derivative of the function to the left of the minimum must be negative, and to the right it must be positive. (It is assumed here that the minimum is at an interior point on the curve.) For a function with continuous first derivative, this leads to the requirement that the derivative at the minimum be zero. In the present case, (the function Q(h) for fixed V), the function is continuous but not necessarily smooth, and the minimum is at an interior point.

Recall that Q is the product of the stoichiometric fuel-flow rate Q_s and the throttle setting. To avoid confusion with the notation in Chapter Three, η^* will be used here to denote the minimum throttle-setting, be it an equilibrium or a chattering setting, for a specified h (keep in mind that, throughout this discussion, V is fixed). In principle, the variation of Q over altitude can be expressed through the variation of Q_s and η^* over h. This in turn is theoretically possible, as for fixed V both of these are functions only of h.

The derivative of Q(h) will depend upon the derivatives of Q_s and η^*. From basic calculus, the derivative can be expanded as

$$\frac{\partial Q}{\partial h} = \frac{\partial \eta^*}{\partial h} \times Q_s + \eta^* \times \frac{\partial}{\partial h}(Q_s). \qquad (7)$$

As the only factor of importance about the derivative is its sign, one would expect that enough information could be garnered to make some fairly conclusive statements.

As the values of Q_s and η^* are calculated in the main from tabular functions, it is not possible to characterize them or their derivatives mathematically. They are instead computed and shown graphically.

Some fairly solid observations about $\partial Q_s/\partial h$ can be made, if only for the particular missile examined, due to the relatively simple dependence of Q_s upon altitude. As it depends directly upon air density, which decreases rapidly with altitude for the relatively low altitudes under consideration,

it is to be expected that the derivative will be negative. This is indeed the case, as is shown in Figure 11, which displays the variation of Q_s over altitude. Note that this is only to say that the derivative is in general negative; the additional dependence upon M (through the capture ratio function) prevents any conclusive statements about its character. Further, it is conceivable that the capture ratio as a function of M for other missiles would vary so sharply that $\partial Q_s/\partial h$ could be positive for some altitudes.

Figure 12 shows the T - D curves for four altitudes at a fixed velocity, and η^* for each curve. (While D_{eo} varies with altitude, it is effectively constant over such small ranges as are considered here.) Note that the curves are quite similar. It is especially to be noted that, in the case of the two curves for which $T(\eta^\circ)$ is greater than D, the slope of the line from $(0, -D_{eo})$ to the point on the curve at η° is greater than the slope of the curve itself. This means that η° is the upper chatter point for η^*.

As altitude increases, the curves move downward on the graph. At some particular point, the thrust at η° equals drag, and thus η° becomes the optimal setting. This is true only because of the previously noted fact that the tangent line is of greater slope than the T - D cubic.

A further result of this variation in slopes becomes apparent as the altitude increases still further. Since $T(\eta^\circ)$ is now less than drag, η_e will be η^*. And this value will

increase more rapidly with altitude than did the chattering η^*. This means that the derivative of η^* with respect to h is not continuous, and thus $\partial Q_s/\partial h$ is not continuous.

Referring back to equation (7), one observes that the second term will be always negative, as $\partial Q_s/\partial h$ is always negative, and η^* is by definition positive. The first term will be positive when $\partial \eta^*/\partial h$ is positive, and negative otherwise. The actual magnitude of a positive $\partial \eta^*/\partial h$ will determine the sign of $\partial Q/\partial h$ itself.

A graph of $\partial Q/\partial h$ vs. altitude is shown in Figure 13. Note that there are two discontinuities; the first occurs at a very low altitude and corresponds to η^* going from a value greater than η^0 to a value less than η^0. The second is the point at which η^* once again becomes greater than η^0. These points are shown on Figure 14 as the intersections of the line η^0 and the η^* curve on the η - h axes. The portion of the curve below the line consists of chattering settings, and will therefore be referred to as the chattering arc.

It is of particular interest in this case that the derivative of Q at the altitude corresponding to the upper end of the chattering arc is negative, while after the discontinuity it is positive. This means that Q at this altitude is a local minimum, and in fact this value turns out to be the actual minimum for this velocity. The graph of Q vs. h is displayed in Figure 15. The minimum point is obvious, although the discontinuity in its slope is not.

The discontinuity in slope is also not obvious at the point corresponding to the lower end of the chattering arc. This is due to the fact that, at each of these points, the slope of the tangent line in the chattering throttle calculation is not greatly different from that of the T - D curve itself near η^0. Thus the jump in $\partial\eta^*/\partial h$ is not large.

In this study, the jump at the upper end of the chattering arc is large enough to bracket zero, and thus the value of Q^* for low velocities is found at the corresponding altitude. Further, this bracketing gives some robustness to this value of η^*. For at least some neighborhood of the flight conditions (velocity and vehicle weight) that generate this result, the value of η^* will not change. It is this robustness that accounts for it being the result for all velocities below V_b.

It should be emphasized that this explanation for the coincidence of η^* and η^0 is based upon strictly local effects. That is to say, the similarity of the curves in Figure 12 is used, but this similarity is a result of the relatively narrow band of altitudes for which these curves were generated. It is not to be assumed that the curves retain their similarity as the altitude band widens, nor for that matter even that they continue to move downwards with increasing altitude. In fact, the lower end of the chattering arc is a result of their moving upward with increasing h, for very low altitudes.

CONCLUSION

DISCUSSION OF RESULTS

The addition of the the Mach-altitude limit to the inequality constraints (2) on the system had a marked effect on the results, in that it provides a sharp constraint upon the maximum velocity achievable. The thermal-choke limit had a great deal of effect on the performance of the missile at very low velocities. As these velocities are below that at which the absolute minimum of the $Q^*(V)$ curve occurs, however, they are not of interest in the optimal control problem.

In both the constrained and the unconstrained cases, the curve of minimum fuel-flow rate vs. velocity was found to be non-convex. This leads to the existence of non-unique solutions to the control problem, should the multipliers in the Hamiltonian (which depend upon those in the performance index) have a certain ratio. More importantly, it leads to the concept of time-sharing between two operating points, to achieve an average velocity between these points.

It has been shown that the non-zero minimum throttle setting, with the accompanying possibility for chattering settings, produces a discontinuity in the slope of the fuel-flow rate vs. altitude curve for a fixed velocity. For the mis-

sile modeled in this study, this discontinuity bracketed zero, and the corner was the minimum fuel-flow rate for that velocity. This is not felt to be a generic result; other missiles may not demonstrate this behavior.

Chattering throttle-settings allow for steady-state operation in a large portion of the flight envelope that is not accessible using constant-operation throttle-settings. Note that throttle-chattering is necessary in this region only due to the requirement that thrust equal drag; this has no effect in the climb phase of a trajectory. The limitations on the flight envelope due to the Mach-altitude and thermal-choke limits must be taken into account in all phases of the trajectory, however.

SUGGESTIONS FOR FURTHER WORK

The existence of a non-convex function of minimum fuel-flow rate versus velocity leads to the possibility of time-sharing between differing altitude-velocity points to achieve optimal performance. It is felt that further study is needed to determine the actual improvement over steady-state flight that is possible through such time-sharing. While some current results [14] indicate that only minimal improvement is to be expected, no work known to the author has been performed in this area using an aircraft of the type studied here.

The model used in this study contained the assumption of constant vehicle-weight, while in actual flight the weight varies appreciably during the trajectory. Different vehicle weights produce different optimal points of operation, and the dynamics of transition from one such point to the next are not included in the reduced-order model. Thus the next step in trajectory optimization for the vehicle in this study would be to study such transition, using a higher-order model. Work has been done in this direction [3, 15], but the inclusion of varying vehicle weight has yet to be performed.

REFERENCES

1. Bryson, A. E. and Ho, Y. C., Applied Optimal Control, Revised printing, Hemisphere, 1975.

2. Leitmann, G., An Introduction to Optimal Control, McGraw-Hill, 1966.

3. Cliff, E. M., Kelley, H., J., and Lutze, F. H., "A Study of Systems Optimization Applied to Surface-to-Air Missile Operations", Report to NSWC, VPI&SU., March, 1985.

4. Bryson, A. E., Desai, M. N., and Hoffman, K., "Energy-State Approximation in Performance Optimization of Supersonic Aircraft", Journal of Aircraft, Vo. 6, Nov-Dec 1969, pp. 481-488.

5. Bilimoria, K. D., Cliff, E. M., and Kelley, H. J., "Classical and Neo-Classical Cruise-Dash Optimization", Journal of Aircraft, July 1985, pp. 555-560.

6. Ashley, H., "Multiple Scaling in Flight Vehicle Dynamic Analysis - A Preliminary Look", AIAA Guidance, Control, and Flight Mechanics Conference, Huntsvile, AL, 1967.

7. Vinh, N. X., Optimal Trajectories in Atmospheric Flight, Elsevier Scientific Publishing Company, 1981.

8. Kelley, H. J., "Aircraft Maneuver Optimization by Reduced-Order Approximation", Control and Dynamic Systems, Vol. 10, C. T. Leondes, ed., Academic Press, 1973, pp. 131-178.

9. Ardema, M. D., "Singular Perturbations in Flight Mechanics", NASA TM X-62 380, August 1974, second revision July 1977.

10. Marchal, C., "Chattering Arcs and Chattering Controls", Journal of Optimization Theory and Applications, Vol. 11, 1973, pp.441-468.

11. Weston, A. R., Cliff, E. M., and Kelley, H. J., "Altitude Transitions in Energy Climbs", Automatica, Vol. 19, 1983, pp. 199-202.

12. Shapiro, A. H., The Dynamics and Thermodynamics of Compressible Fluid Flow, Ronald, New York, 1953.

13. International Mathematics Subroutine Library. Document MT01, User Services Dept., Virginia Tech Computing Center, 1984, Routine ZXGSN.

14. Houlihan, S. C., Cliff, E. M., and Kelley, H. J., "Study of Chattering Cruise", Journal of Aircraft, Vol. 19, 1982, pp. 119-124.

15. Shankar, U. J., "Singular Perturbation Analysis of Climb-Cruise-Dash Optimization", Master's Thesis, Virginia Polytechnic Institute and State University, May, 1985.

APPENDIX A. AERODYNAMIC/PROPULSIVE MODELING

ATMOSPHERE

Air density (slugs/ft^3) and sonic velocity (ft/sec) are supplied in tabular form as functions of altitude (ft). The sonic velocity and the natural logarithm of the atmospheric density are interpolated as cubic-spline functions of altitude.

Resulting graphs of atmospheric density and sonic velocity versus altitude are shown in Figures 16 and 17, respectively. The acceleration due to gravity (ft/sec^2) is a specified constant.

AERODYNAMICS

The principal aerodynamic data are specified in terms of normal and axial force coefficients, C_N and C_X. The normal force coefficient is specified as a tabular function of Mach and angle-of-attack. This data is interpolated by a spline-lattice procedure. Figures 18-20 display typical results.

The axial force coefficient is specified in tabular form as a function of Mach, altitude, and angle-of-attack. Rather than construct a three-dimensional spline-lattice the procedure was to use a two-dimensional spline-lattice to interpo-

late the Mach-altitude dependence of C_X at each value of α for which data were supplied. These values are then fit, in a least-squares manner, to a quadratic of the form

$$C_X = a_0 + a_2\alpha^2$$

so that the slope $C_X(\alpha)$ is zero at alpha equal to zero. The axial coefficient is then evaluated form the quadratic expression. Typical plots of C_X dependence are displayed in Figures 21 and 22.

PROPULSION

Air-flow for the ramjet is calculated from

$$w_a = \rho \times V \times S_e \times AOAI$$

where S_e is the (constant) engine inlet area and AOAI is a Mach-dependent capture ratio. The function AOAI(M) is supplied as a data table and interpolated using the spline procedure previously mentioned. The graph of AOAI vs. M is shown in Figure 23.

Fuel-flow is computed by

$$Q = \eta \times Q_s \qquad (A.1)$$

where Q_s, the stoichiometric fuel-flow, is computed from

$$Q_s = w_a \times FAS/e.$$

Here, FAS is the (constant) fuel-to-air ratio for stochiometric combustion, and e is the (constant) propulsive efficiency.

The throttle-setting η is subject to several limitations. The engine will not operate should η be less than a specified (positive non-zero) minimum value; thus values less than this are inadmissible. The maximum value for η is nominally unity; this is subject to two further limitations.

The first of these is due to the limit of maximum fuel-flow, WFMAX. This is a specified limit, in pounds per second, on the amount of fuel that the delivery apparatus can supply. From the equation for fuel-flow (equation A.1), it is seen that

$$\eta \leq \text{WFMAX}/Q_s.$$

The second limitation is a thermal-choke limit. This is provided as a tabular function of Mach number and altitude, and is evaluated by a cubic spline-lattice fit to the table values. Descriptive curves of this limit are displayed in Figure 24.

Thrust is computed from fuel-flow as

$$T = Q \times I_{sp} \times e. \qquad (A.2)$$

The specific impulse I_{sp} is supplied as a tabular function of Mach, altitude, and throttle setting, η. The I_{sp} is represented by spline-lattice interpolation as a function of Mach and altitude for each tabulated throttle-setting. These values are fit in a least-squares sense by a quadratic function of throttle-setting

$$I_{sp} = w_0 + w_1\eta + w_2\eta^2 \qquad (A.3)$$

A typical graph of I_{sp} is shown in Figure 25.

When the equation for I_{sp} (A.3) is plugged into equation A.2, the result is a cubic equation in η for thrust (h and V fixed). As drag is a constant for fixed h and V, this leads to the creation of the "T - D cubic", which can be solved to give the value of η for which thrust equals drag at a specified altitude and velocity.

The engine inlet is responsible for an axial drag component C_{Xi}. These values are given in tabular form as a function of Mach, and these data are interpolated by a cubic spline. The graph of C_{Xi} vs. Mach is displayed in Figure 26.

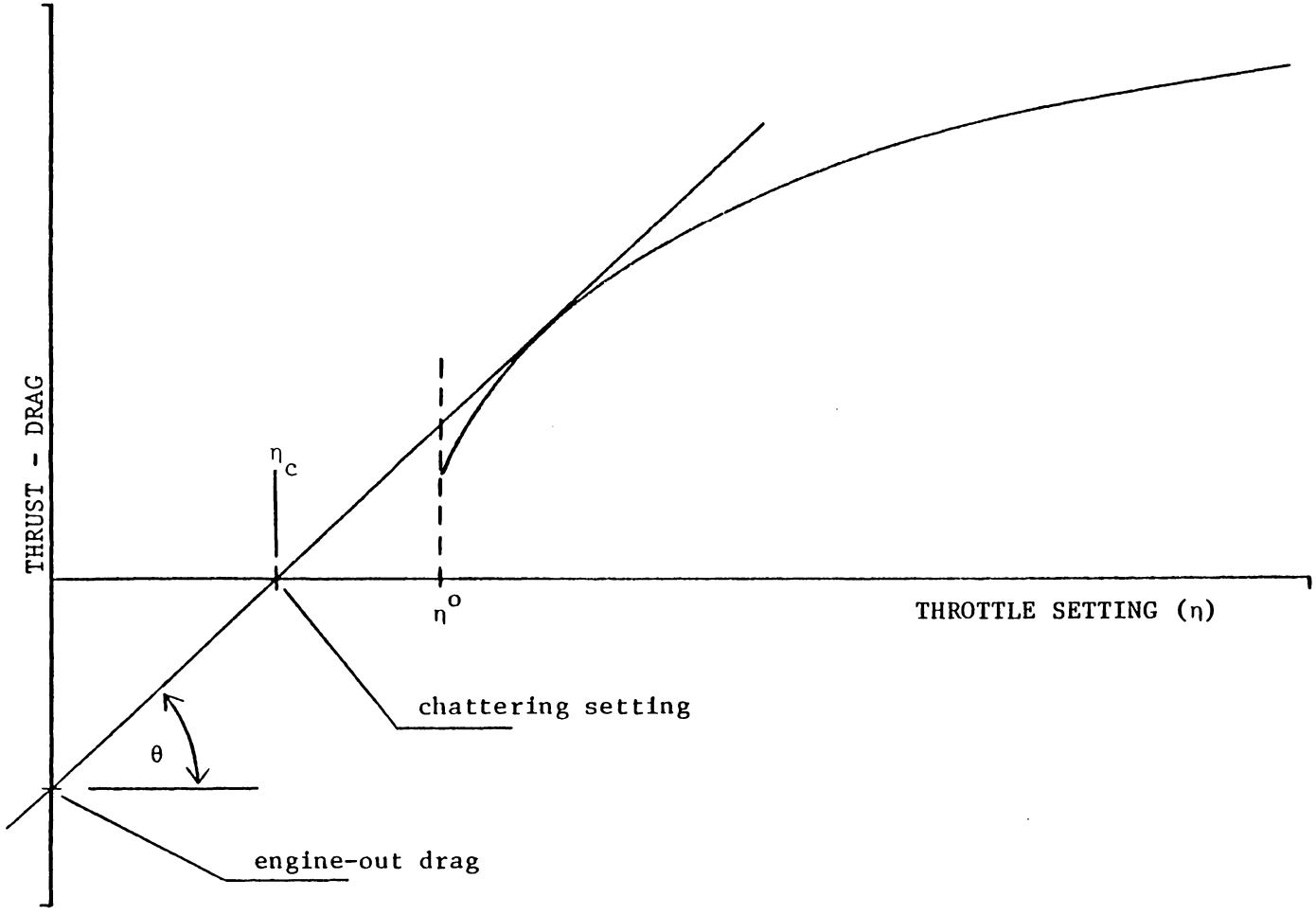

Figure 1. Calculation of chattering throttle-setting.

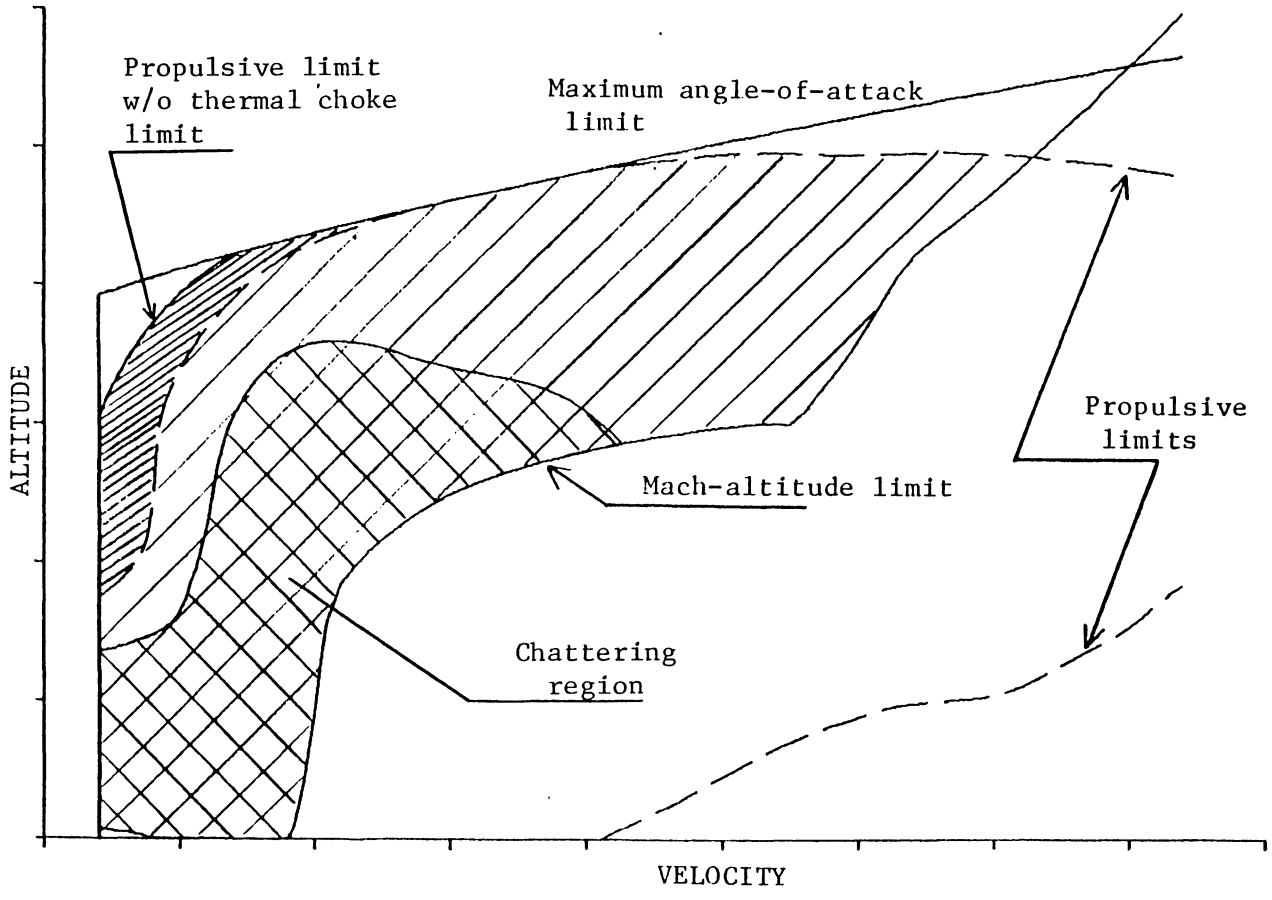

Figure 2. Flight Envelope.

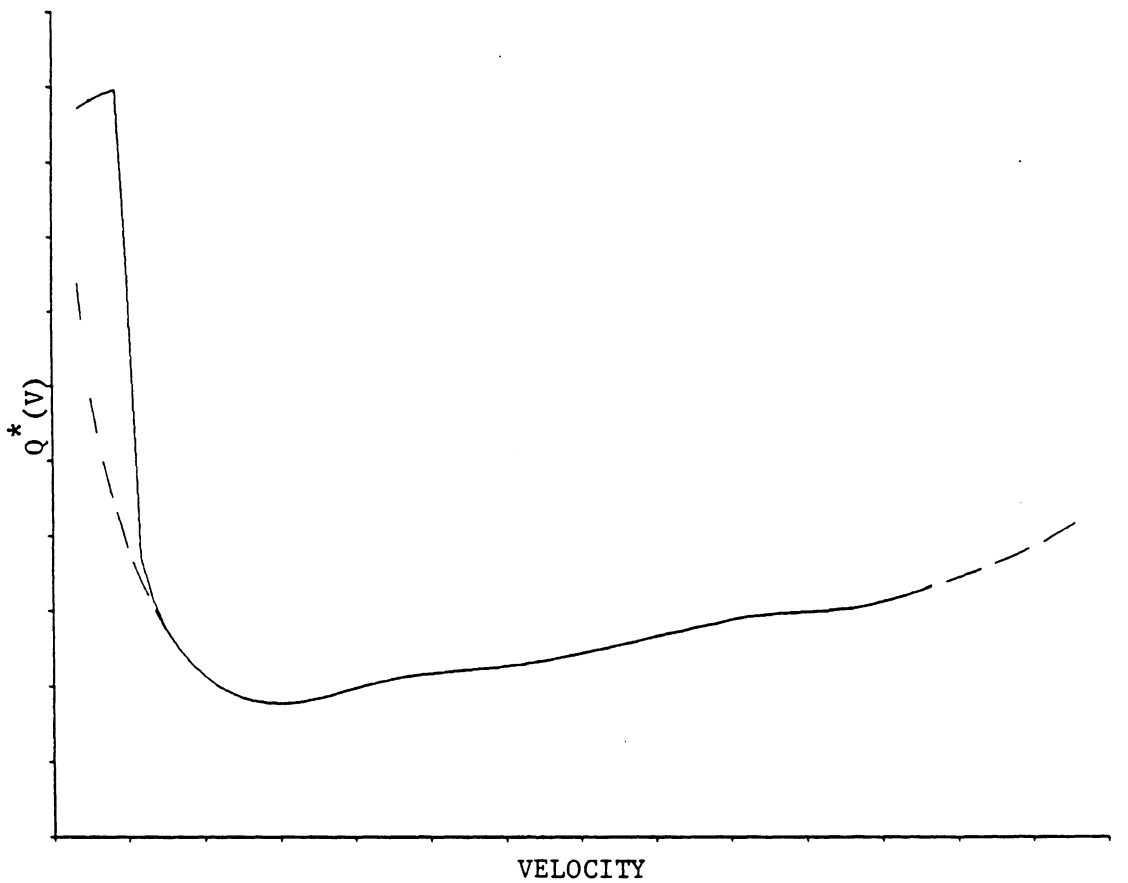

Figure 3. $Q^*(V)$ for typical cases.

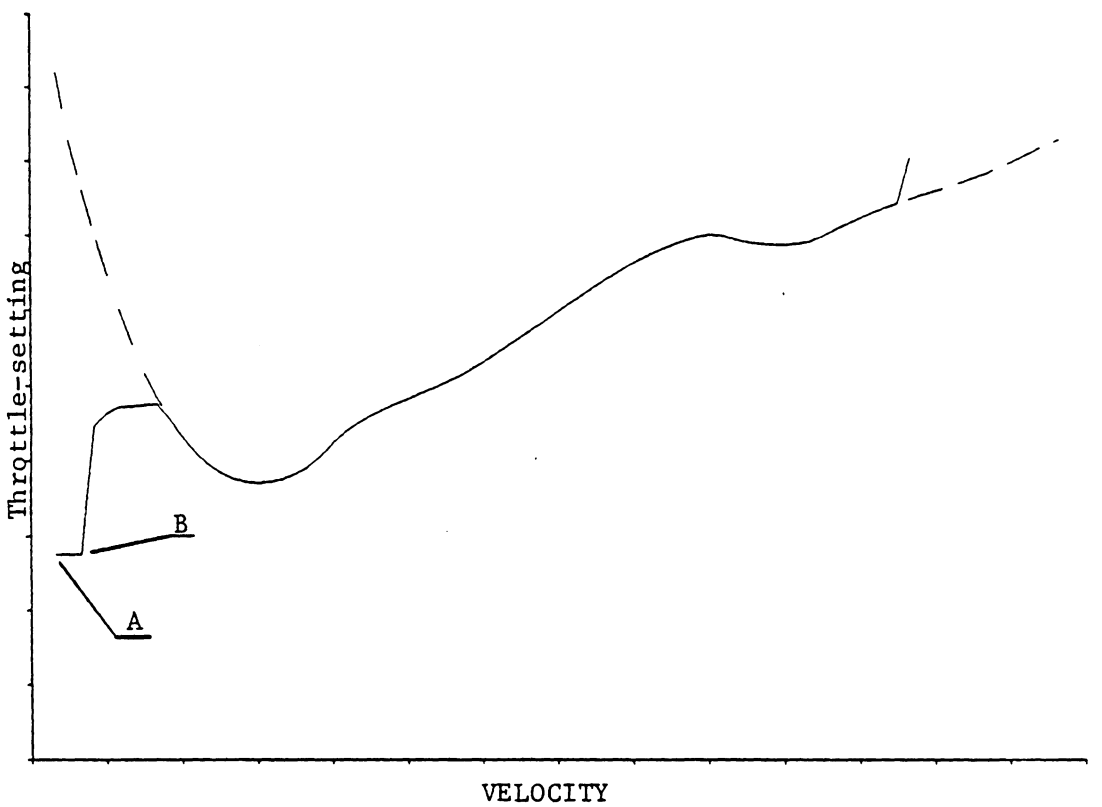

Figure 4. Throttle-Setting for $Q^*(V)$ for typical cases.

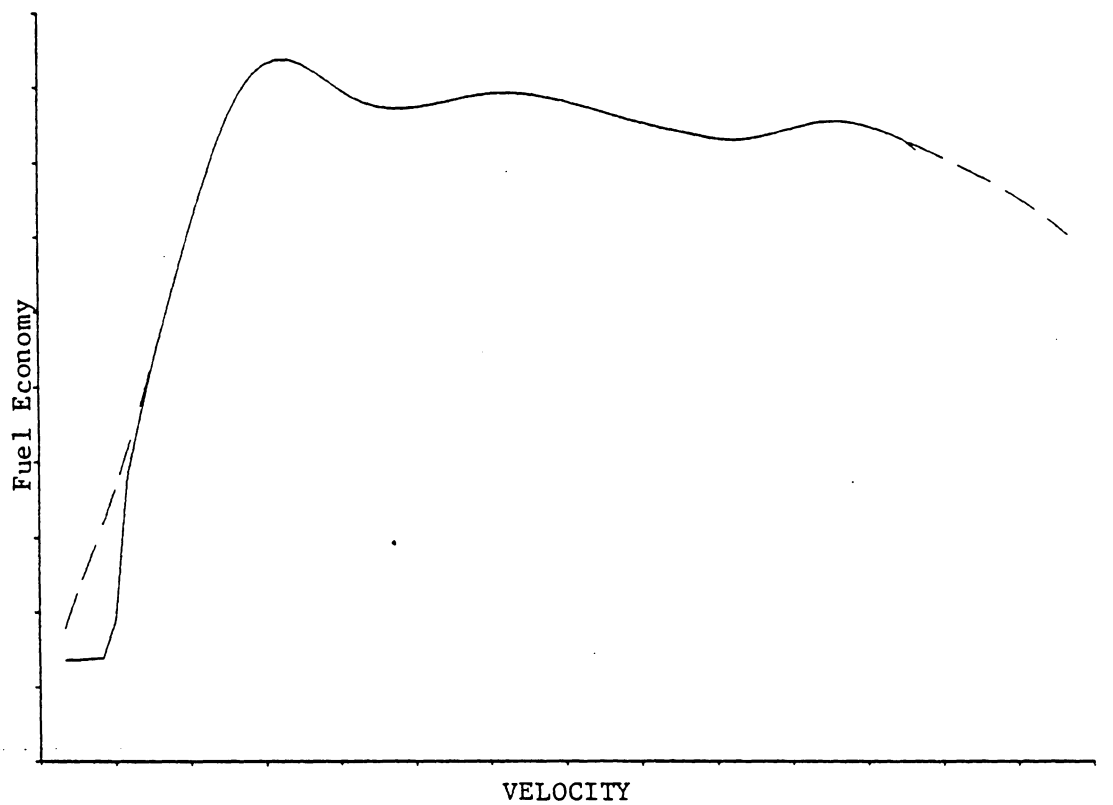

Figure 5. Fuel economy for $Q^*(V)$ for typical cases.

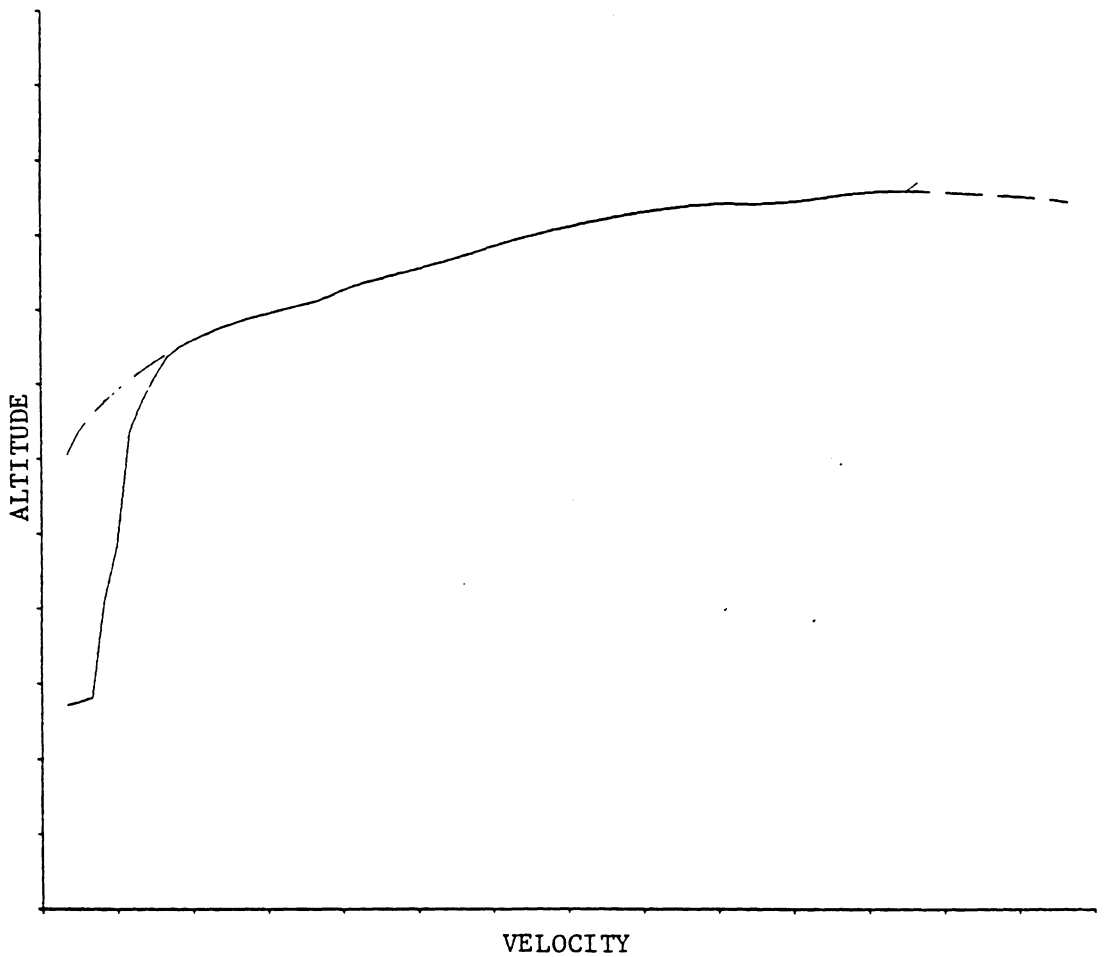

Figure 6. Altitude for $Q^{*}(V)$ for typical cases.

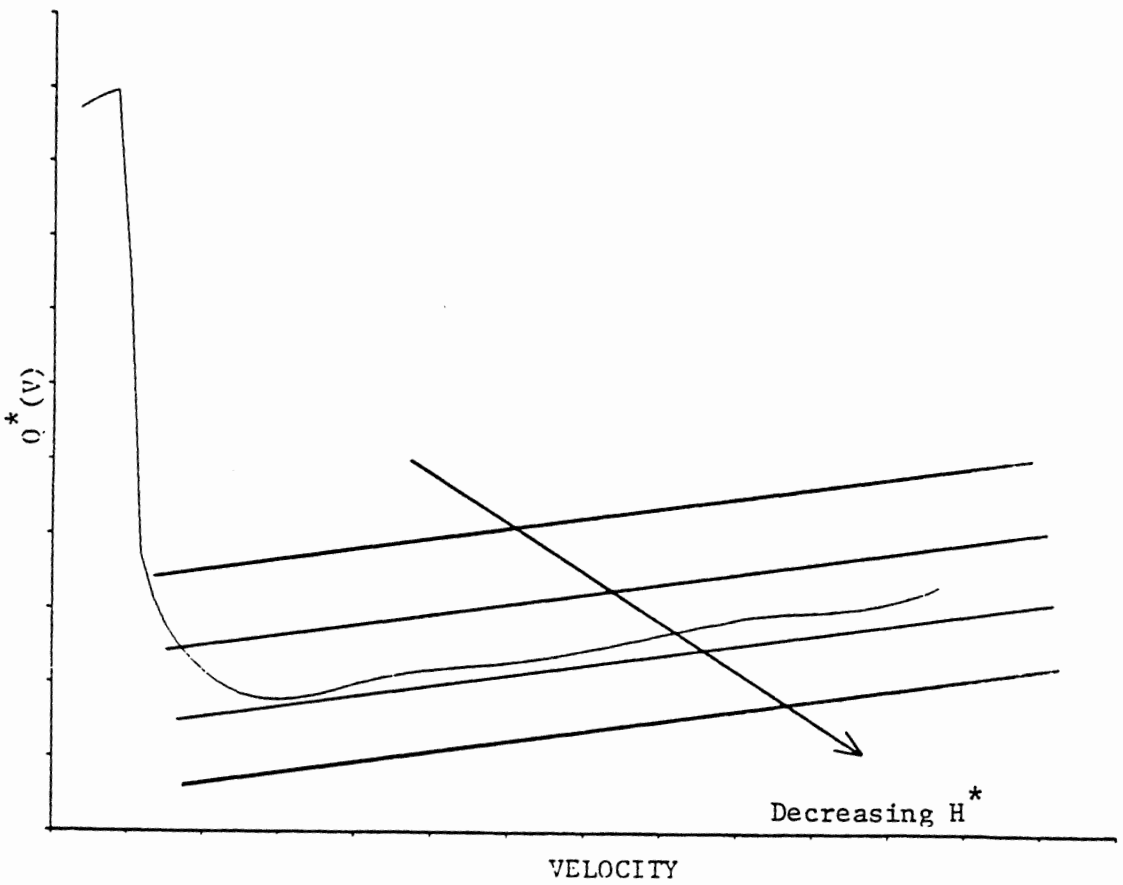

Figure 7. Characterization of results.

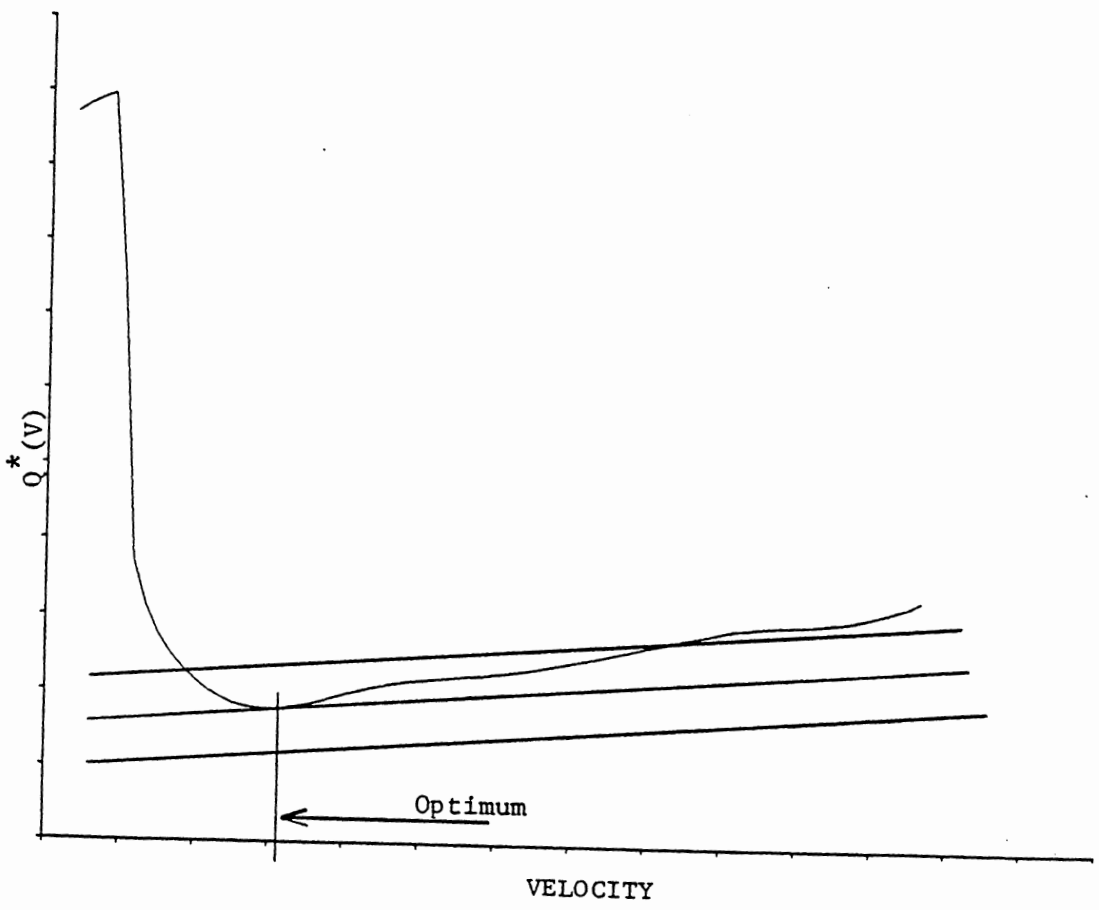

Figure 8. $Q^*(V)$ vs. V with lines of constant H (λ_F large).

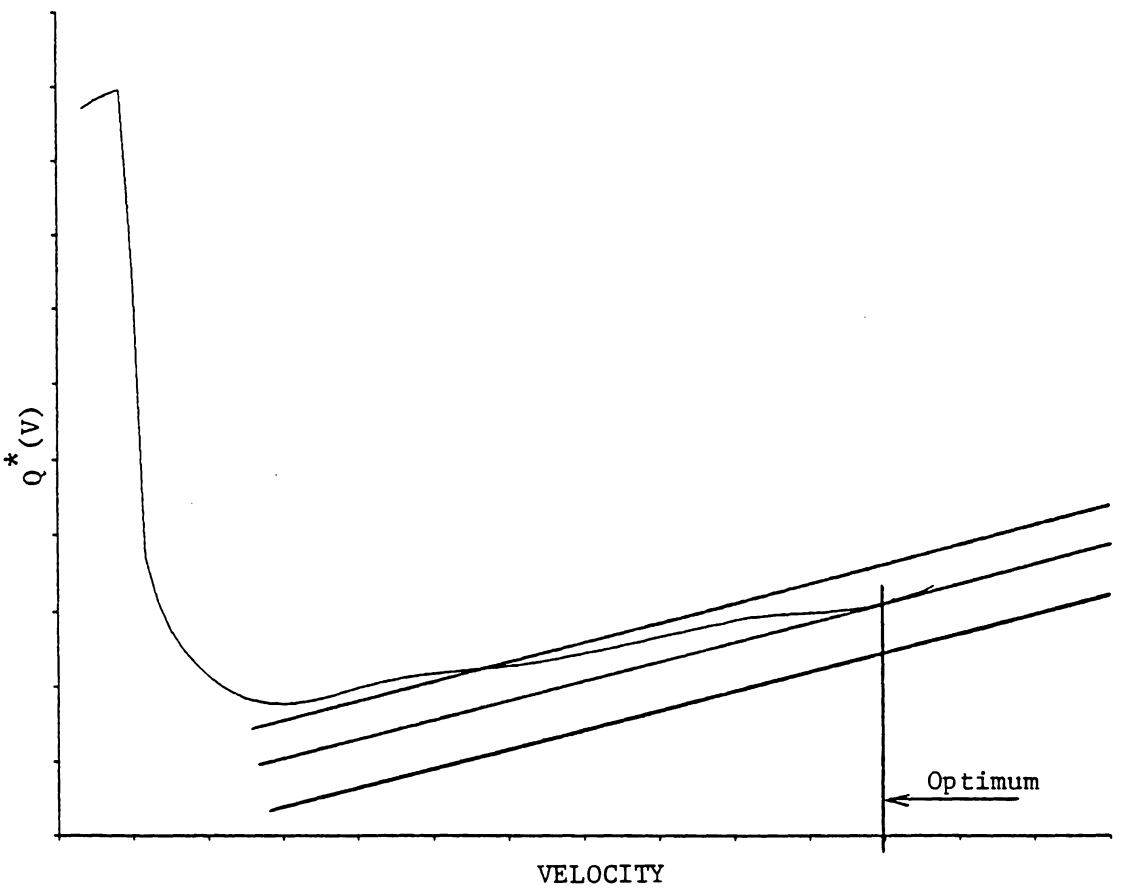

Figure 9. $Q^*(V)$ vs. V with lines of constant H (λ_R large).

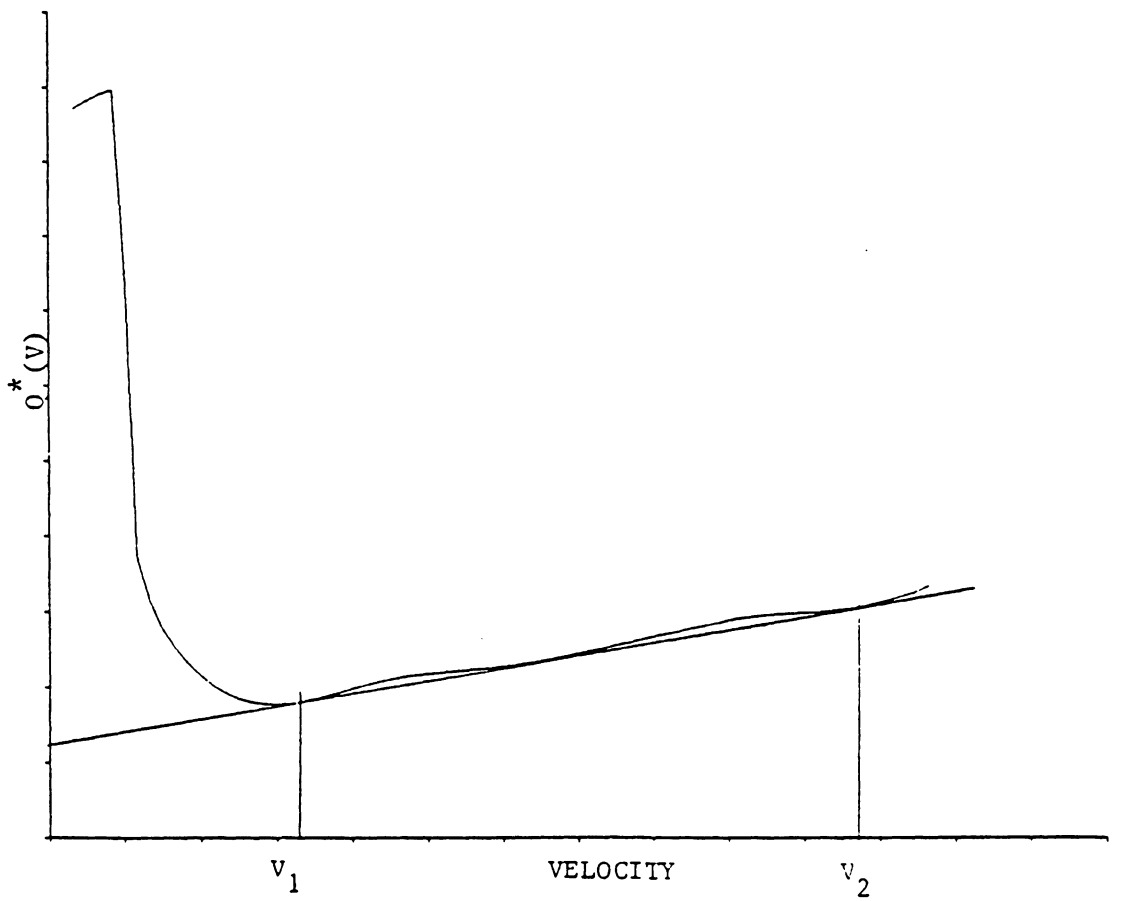

Figure 10. $Q^*(V)$ vs. V with supporting hyperplane.

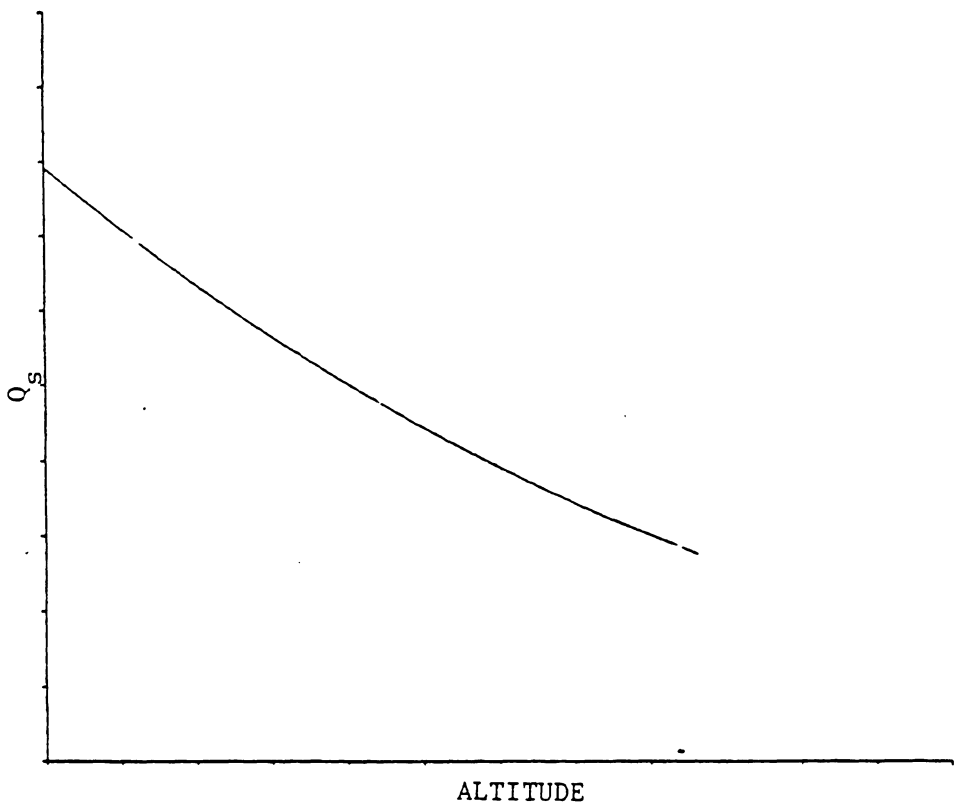

Figure 11. $Q_s(h)$ for fixed V.

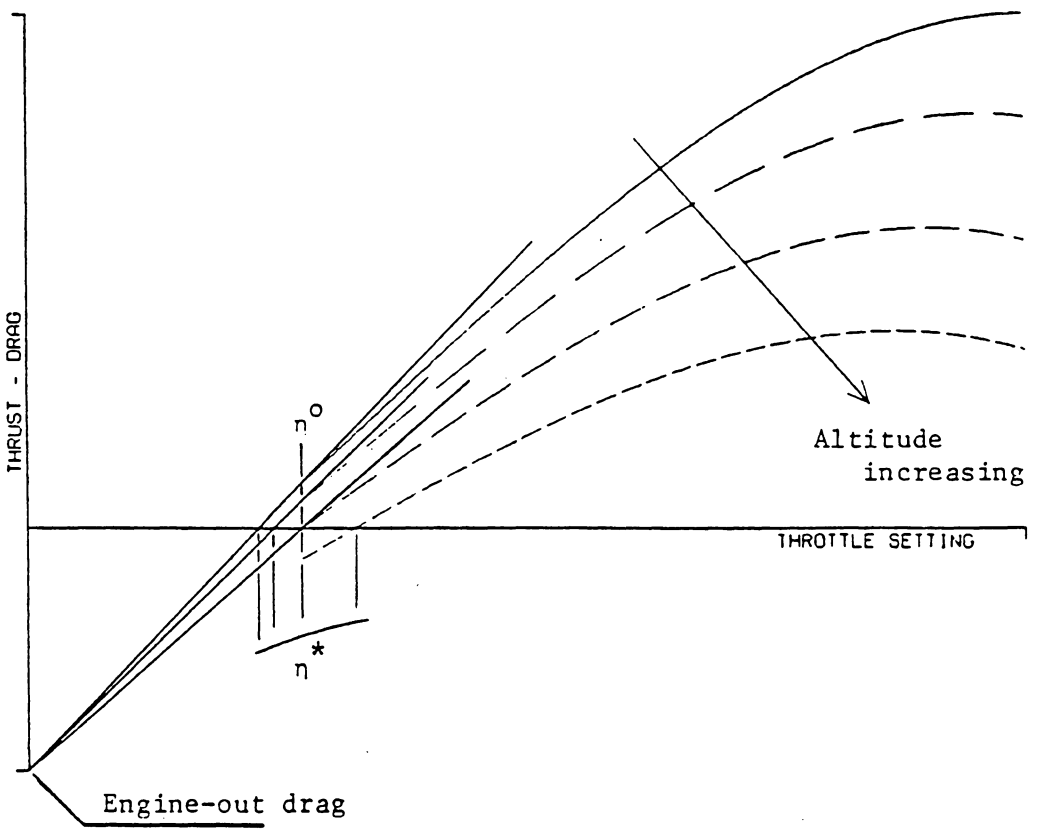

Figure 12. Variation of T-D and η* with altitude (fixed V).

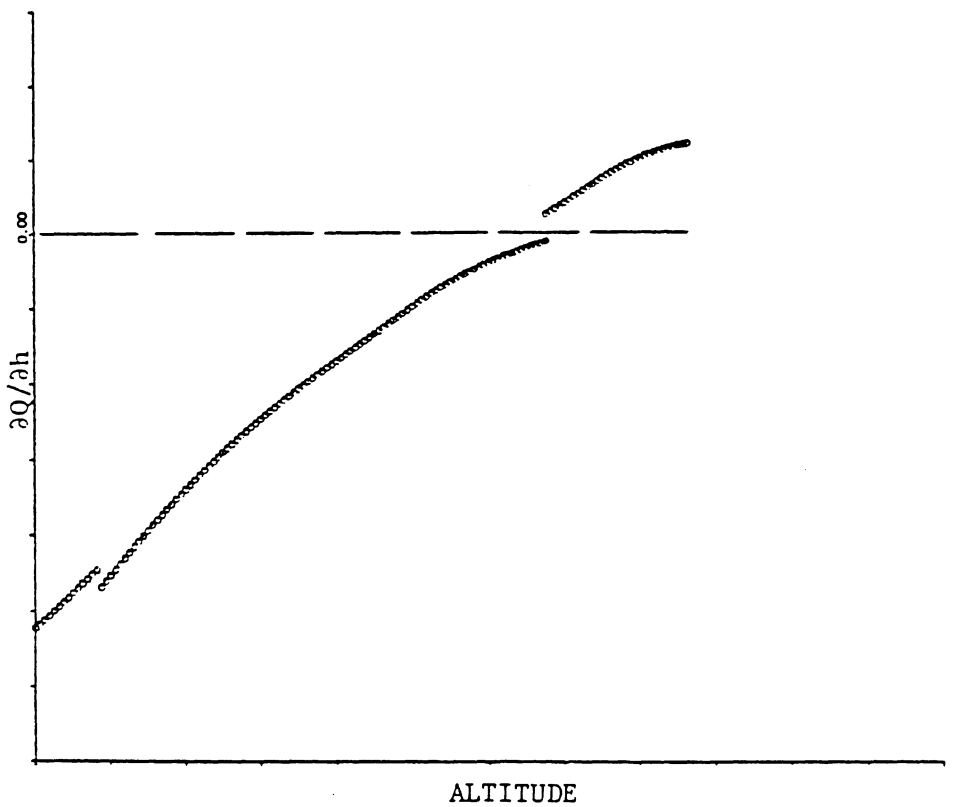

Figure 13. Partial derivative of Q w.r.t. h vs. h (fixed V).

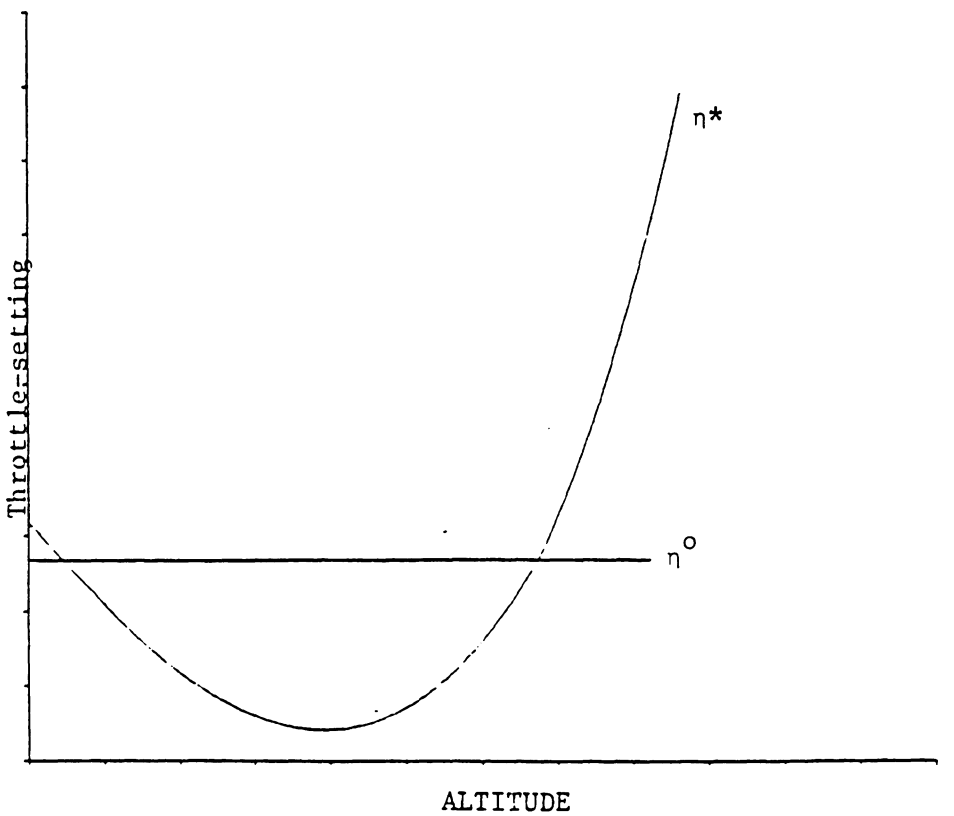

Figure 14. η* vs. h (fixed V).

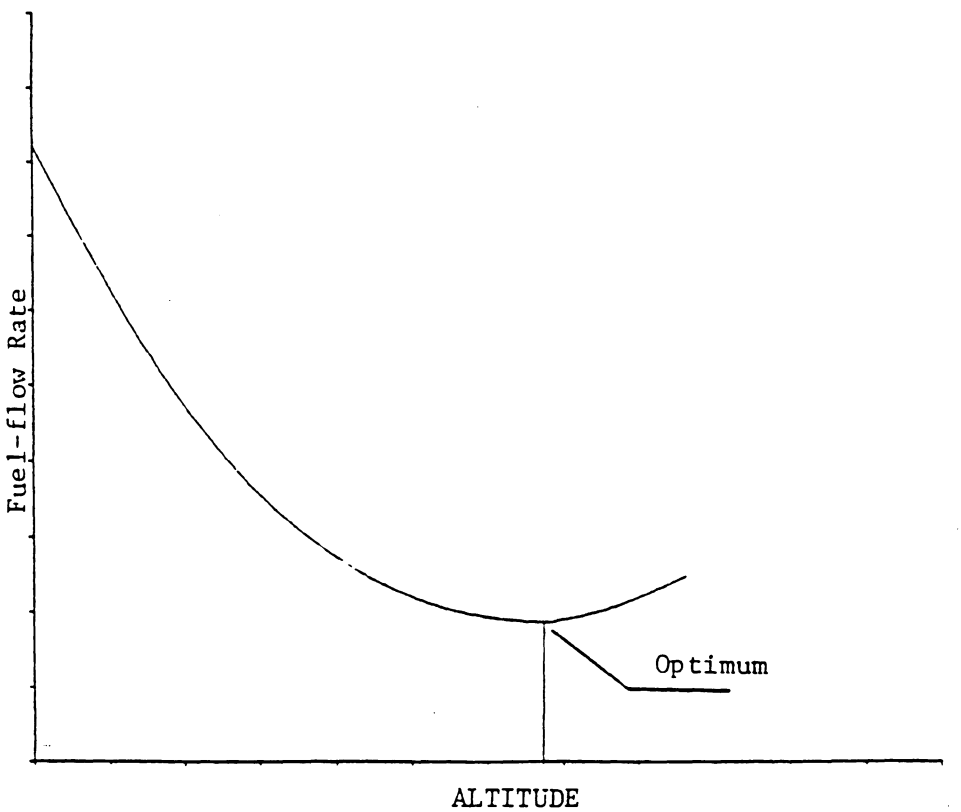

Figure 15. Fuel-flow rate vs. altitude (fixed V).

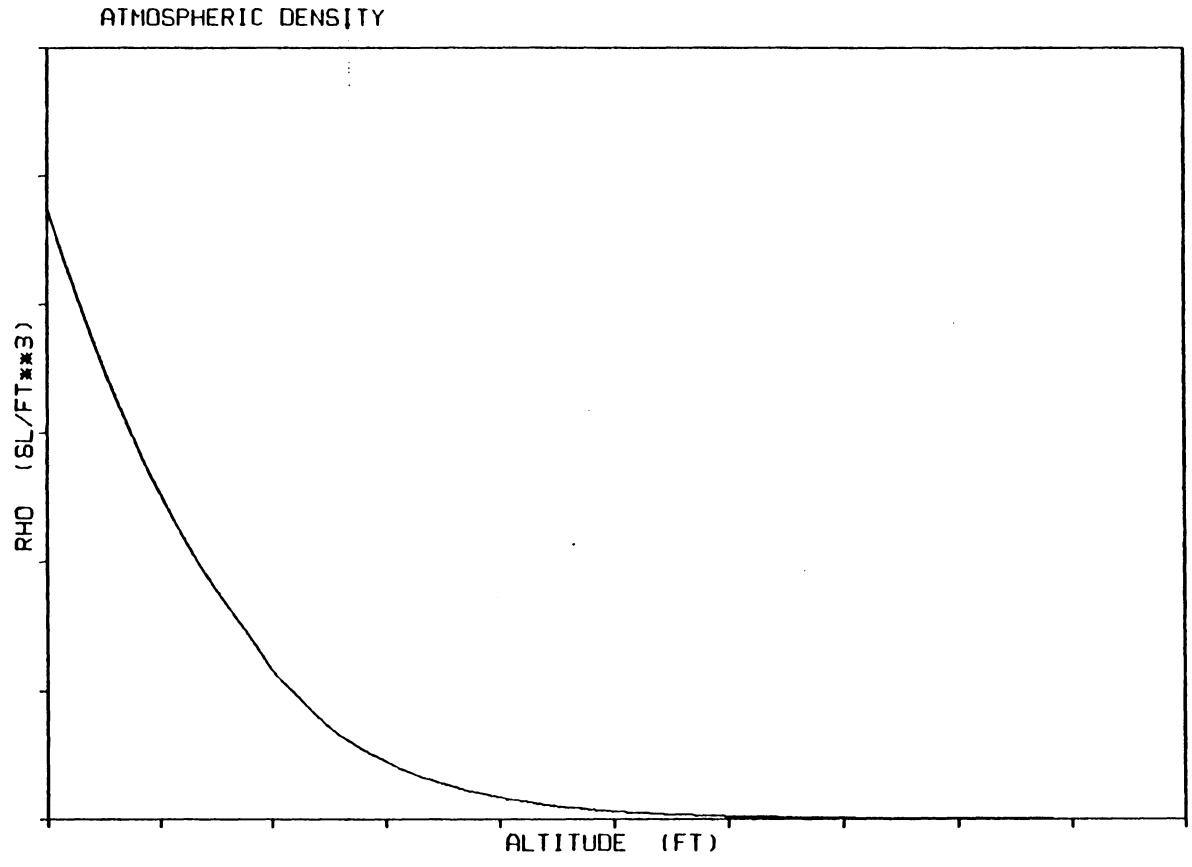

Figure 16. Air density vs. altitude.

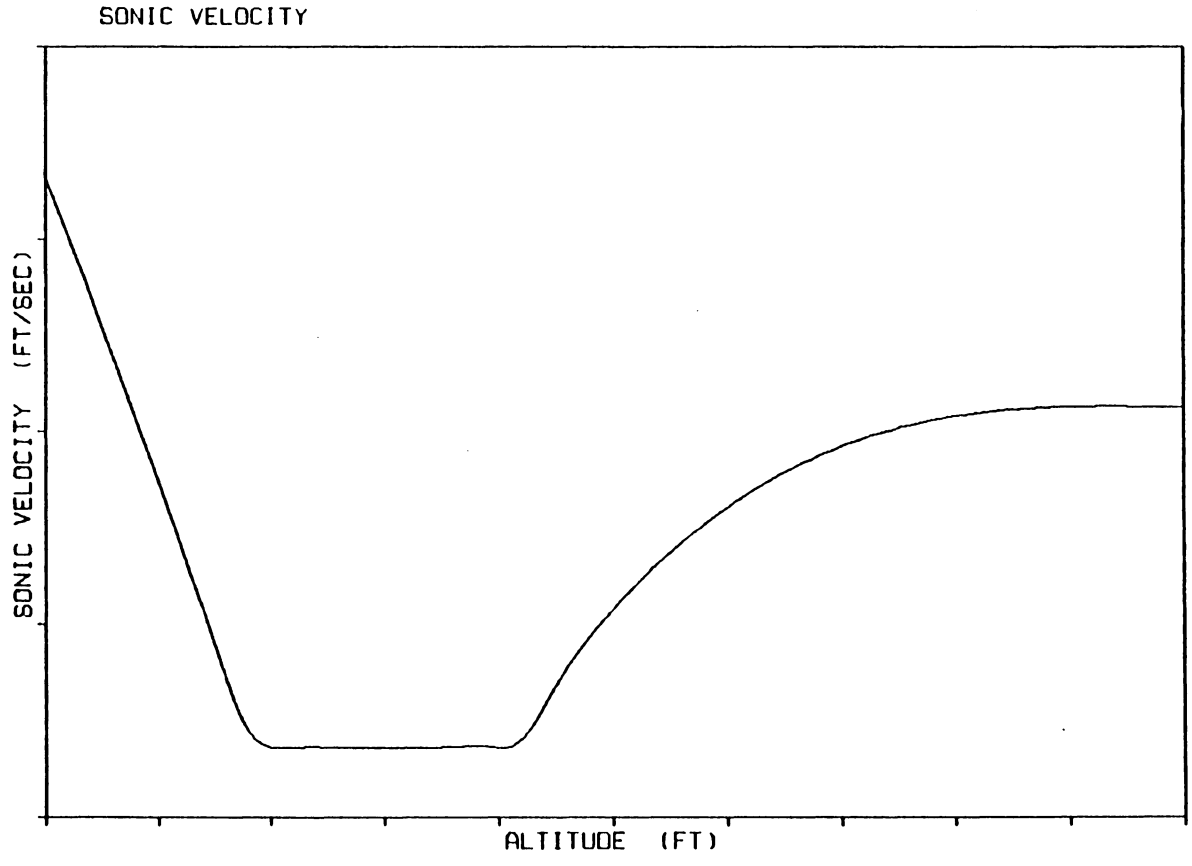

Figure 17. Sonic velocity vs. altitude.

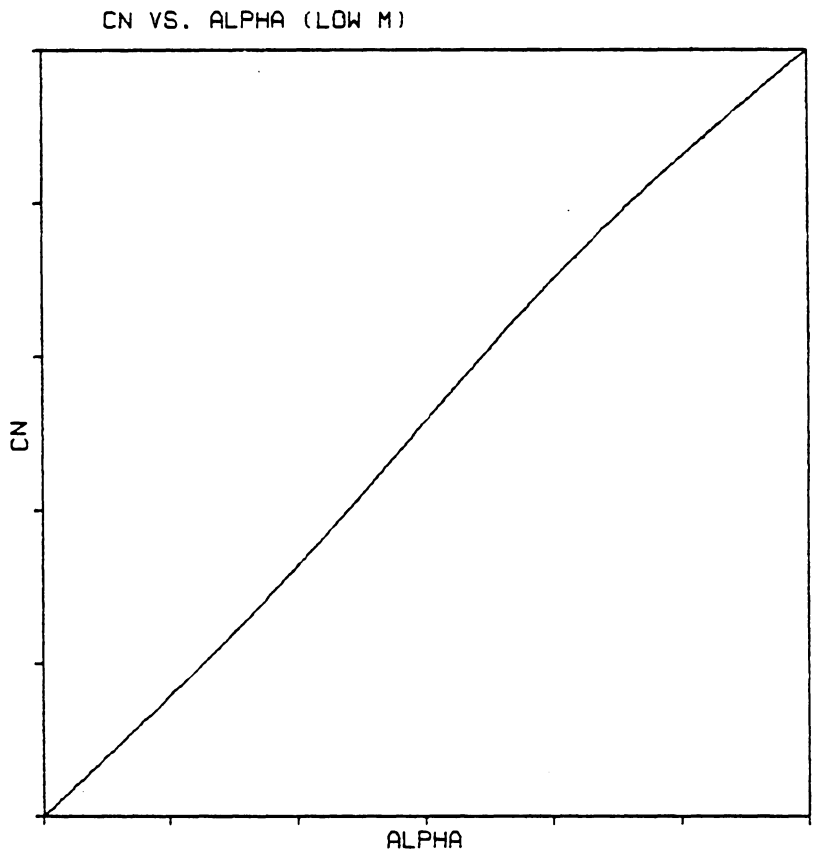

Figure 18. Normal Force Coefficient vs. Alpha (low M).

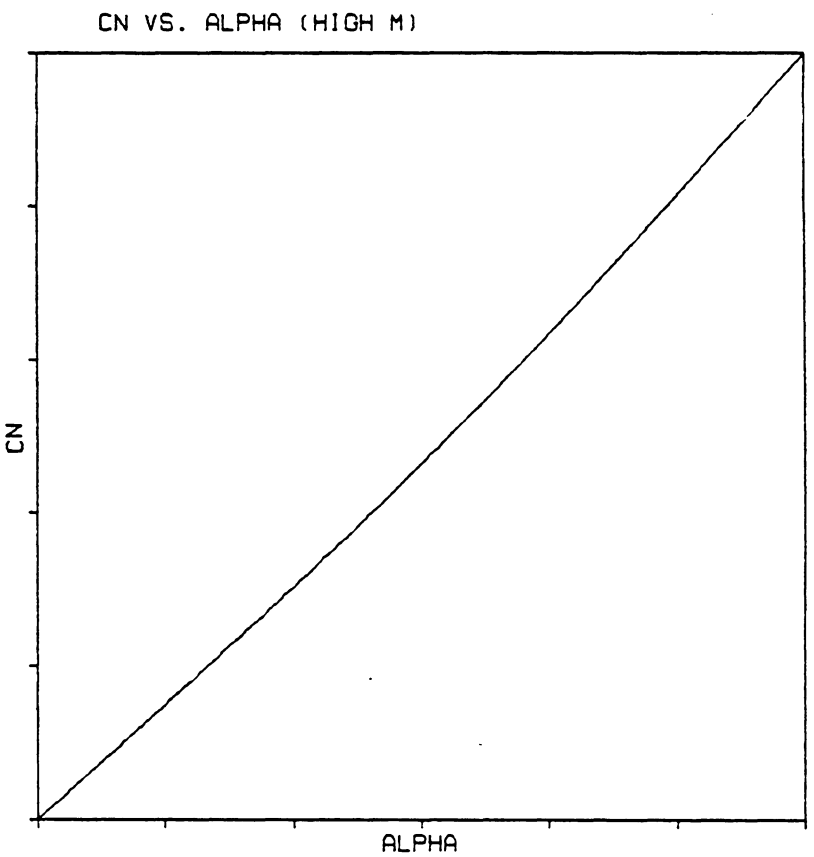

Figure 19. Normal Force Coefficient vs. Alpha (high M).

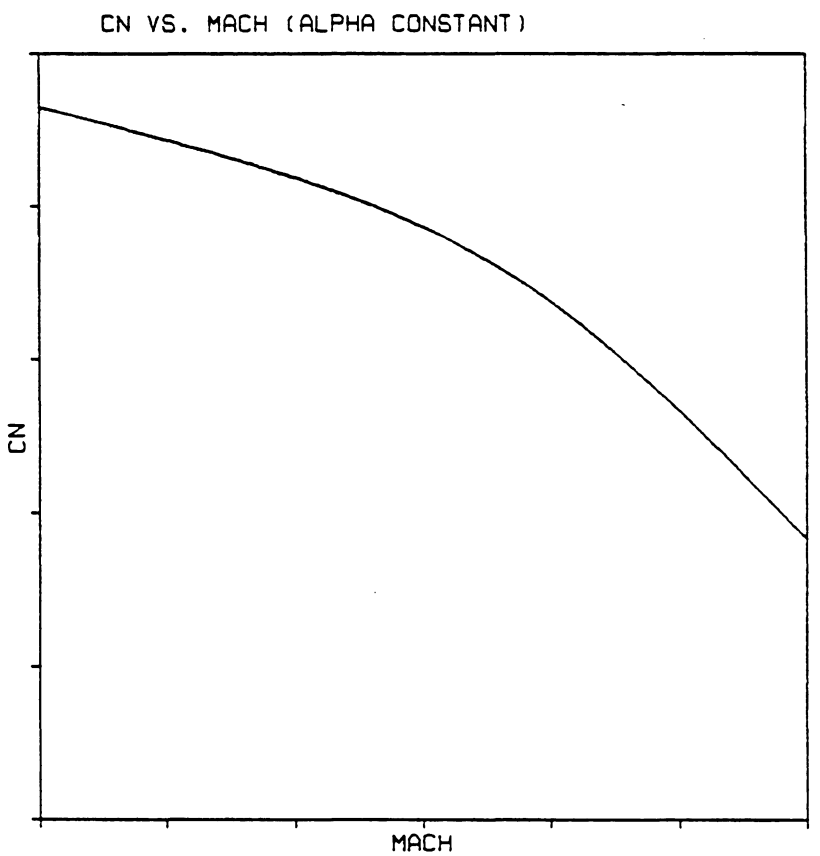

Figure 20. Normal Force Coefficient vs. M (alpha fixed).

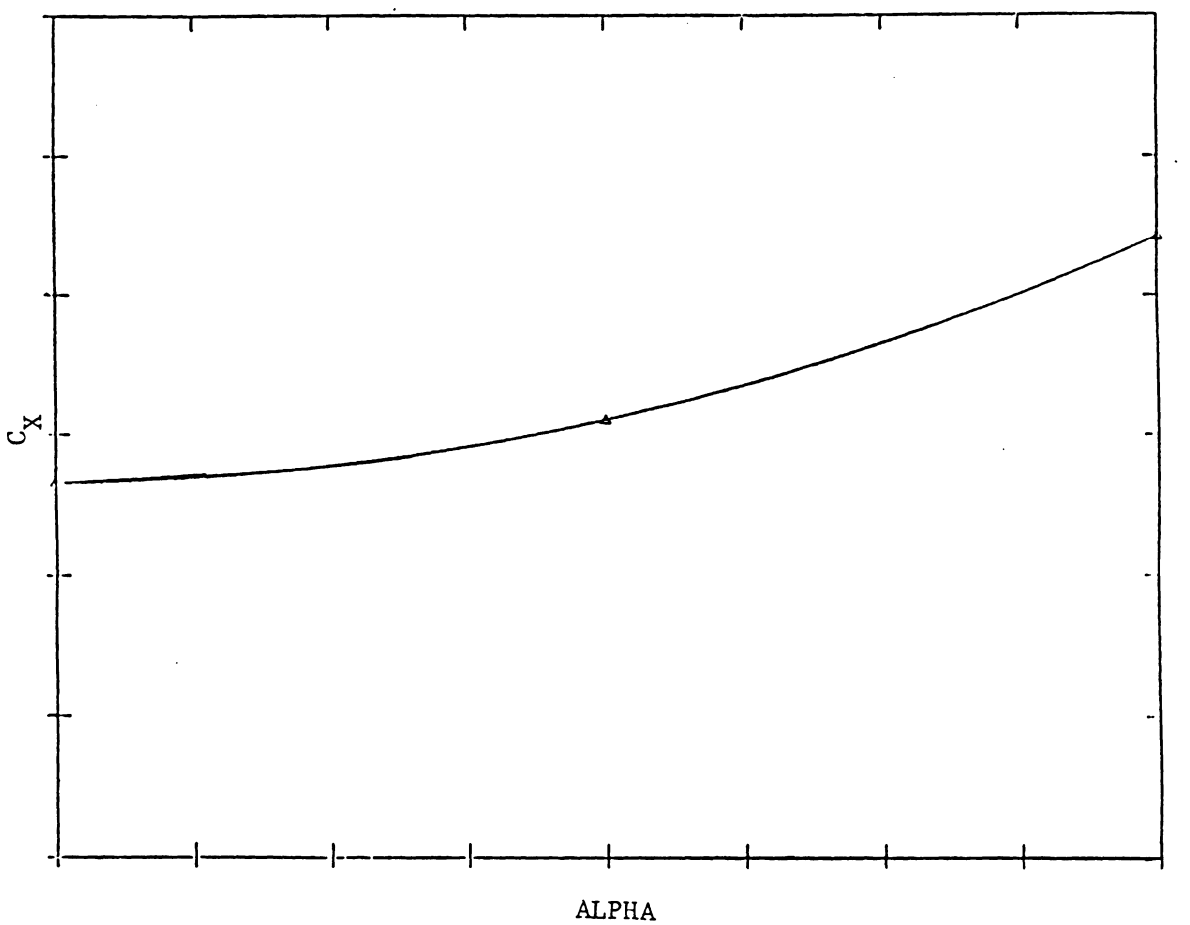

Figure 21. Axial Force Coefficient vs. Alpha (M fixed).

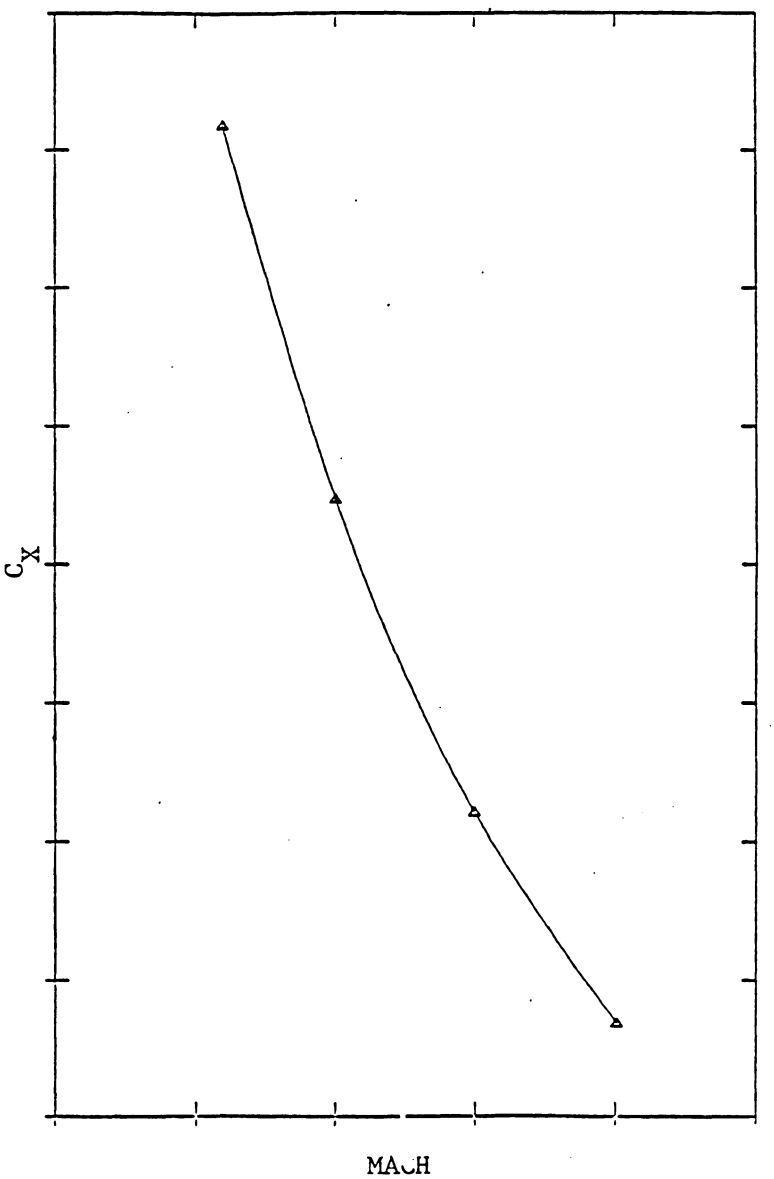

Figure 22. Axial Force Coefficient vs. M (alpha fixed).

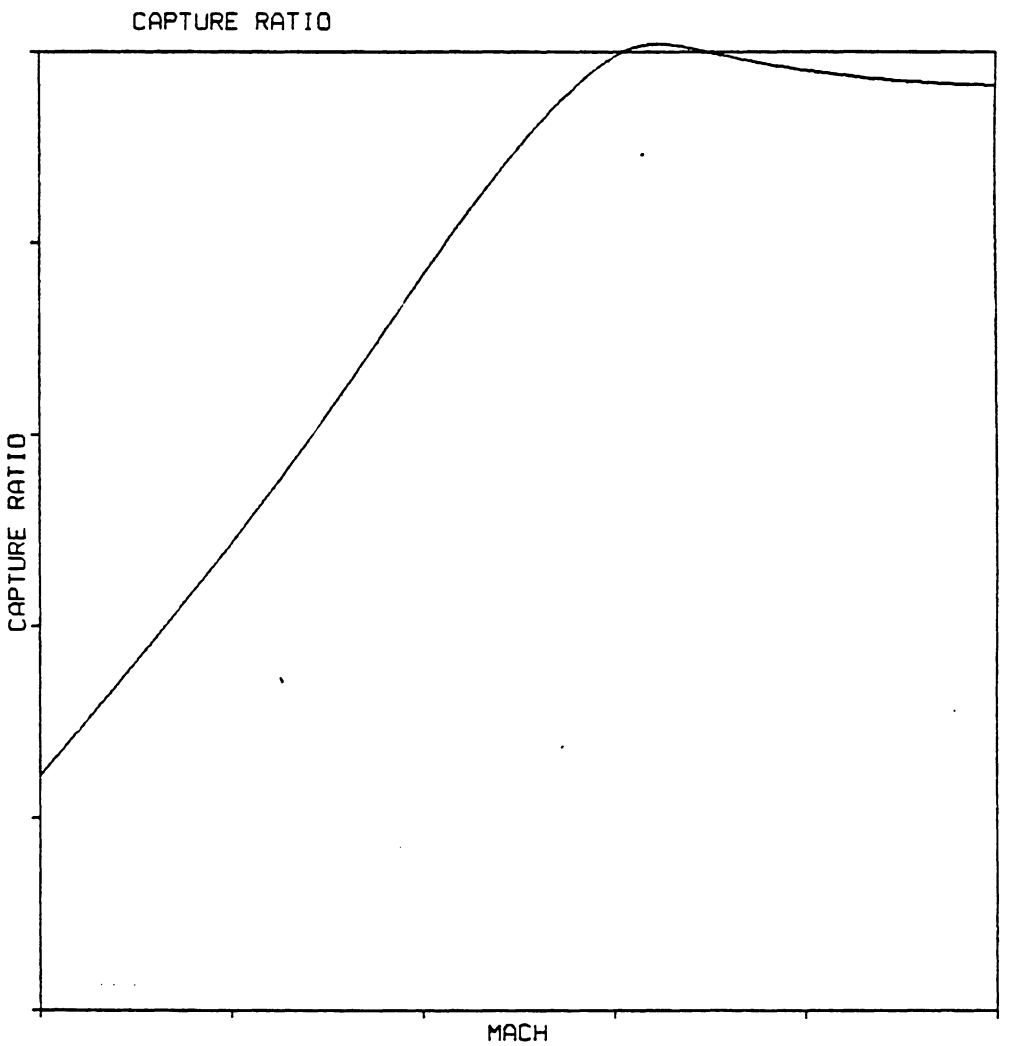

Figure 23. Capture Ratio vs. Mach number.

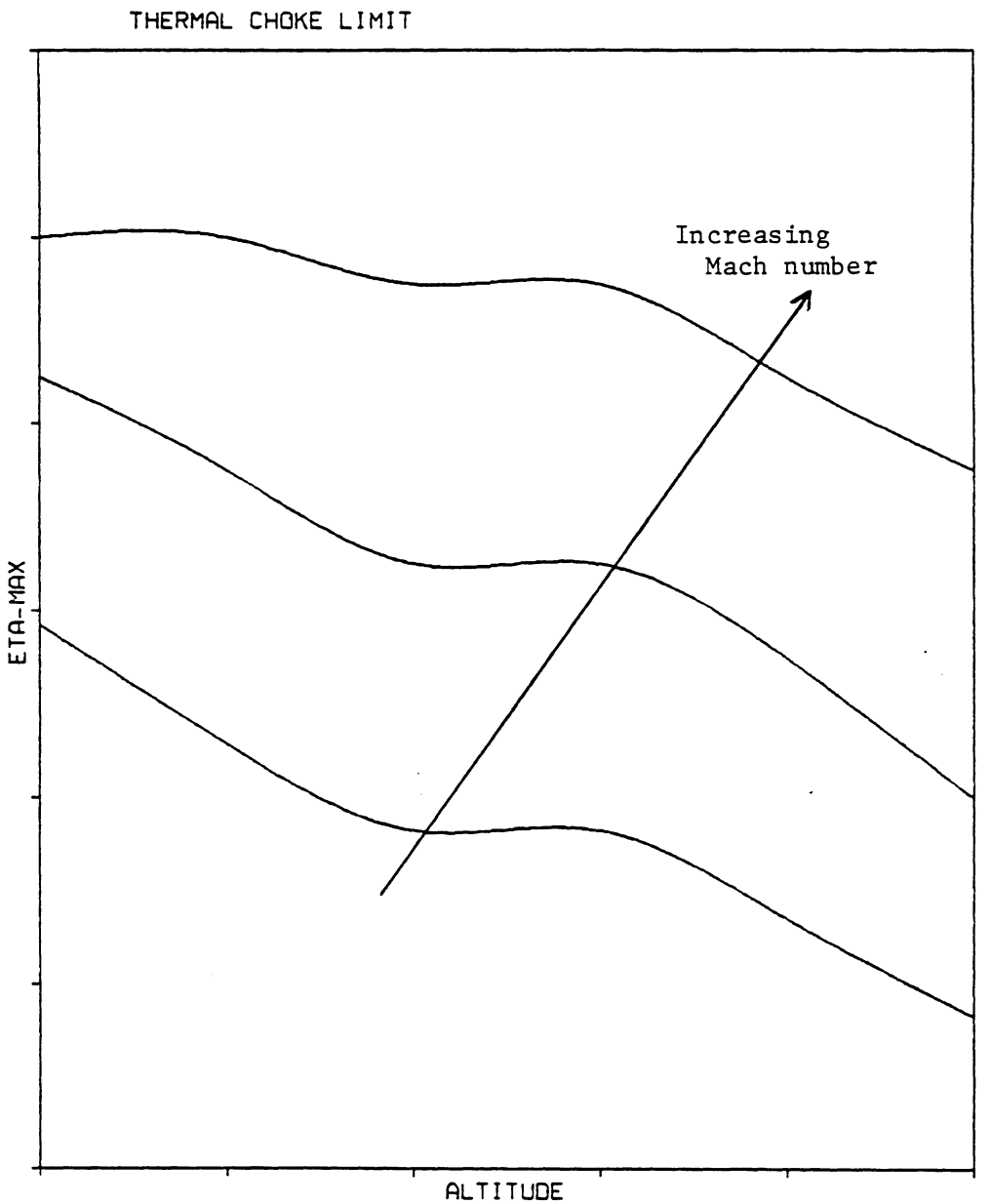

Figure 24. Thermal Choke Limits on Throttle-Setting.

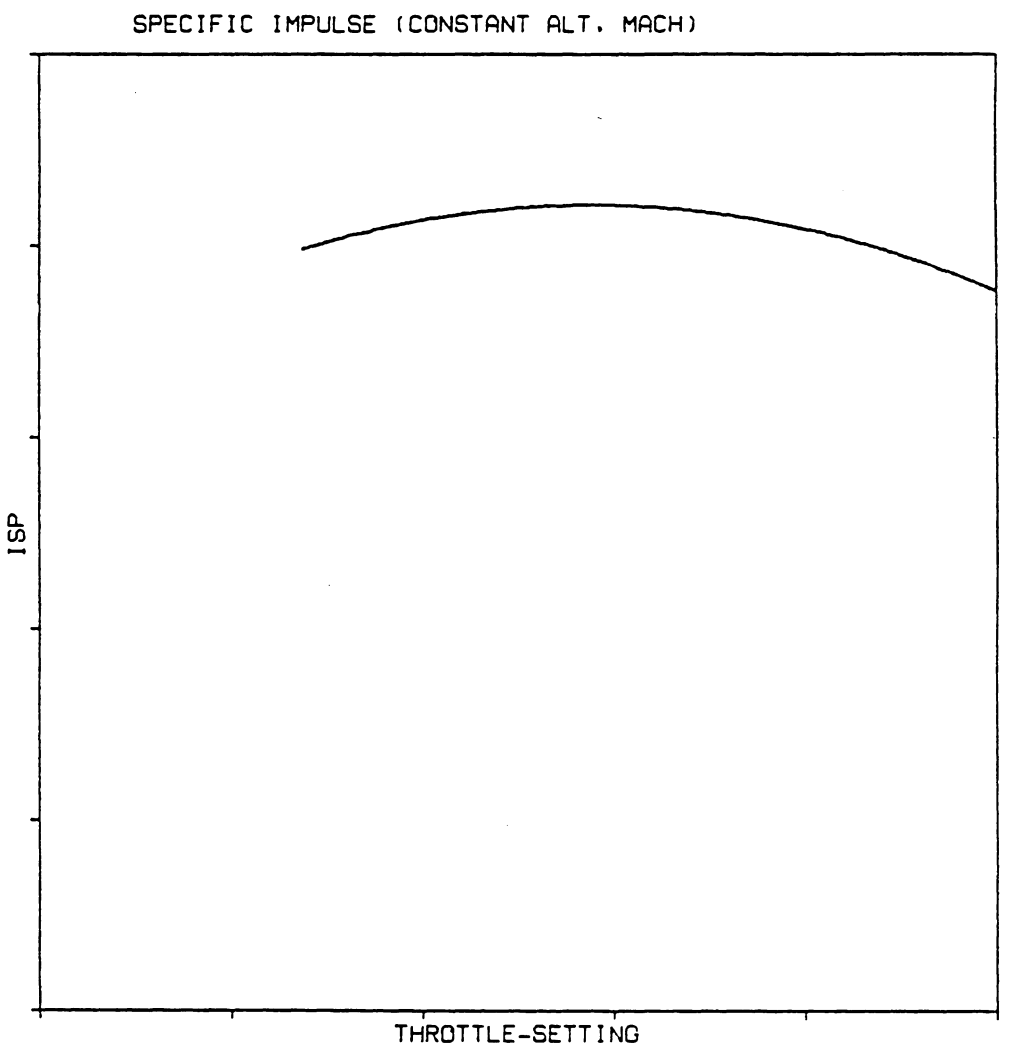

Figure 25. Thrust Specific Impulse (fixed M, h)

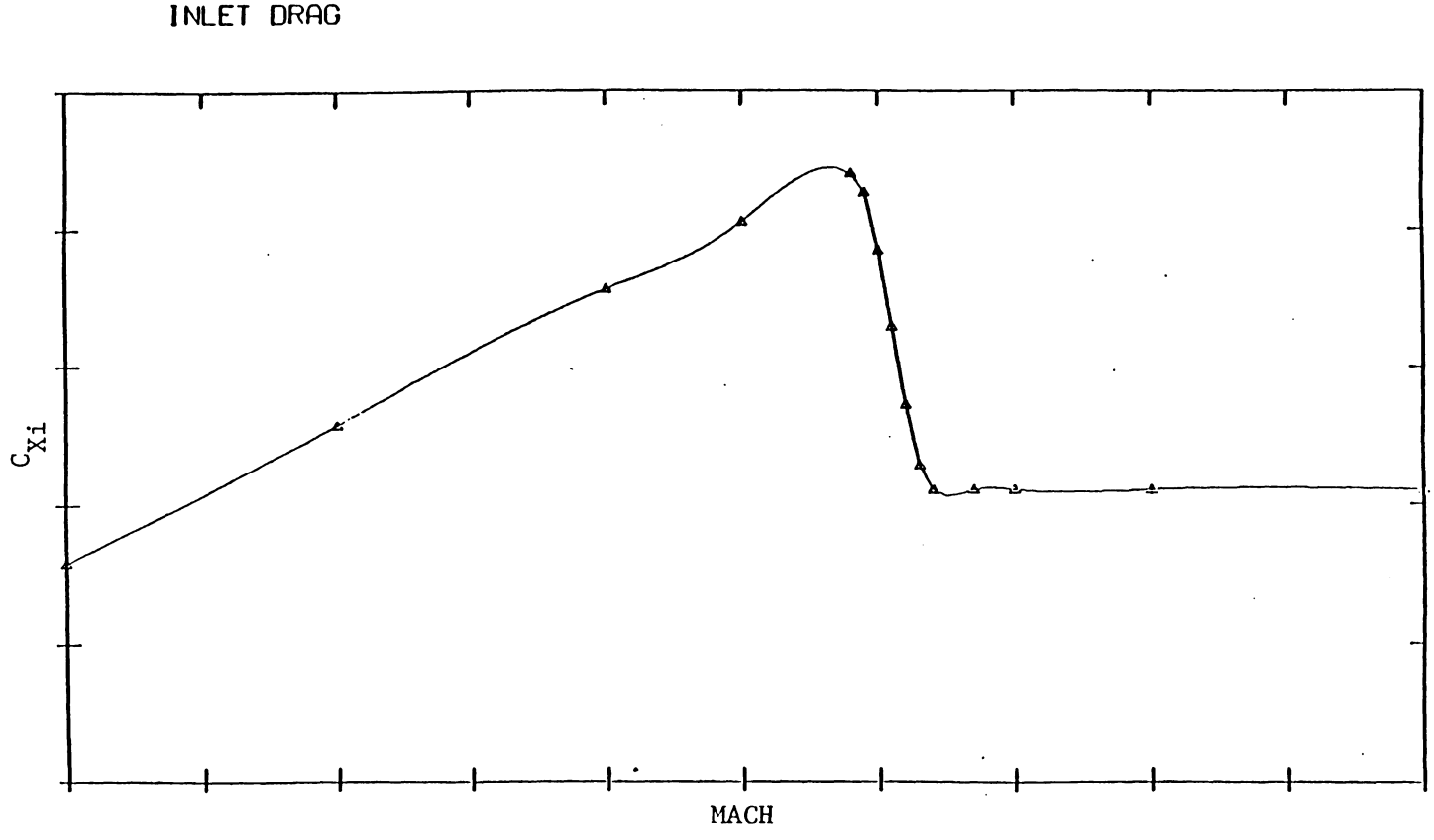

Figure 26. Inlet Drag Increment vs. M.

The vita has been removed from the scanned document